

ac-driven vortices and the Hall effect in a superconductor with a tilted washboard pinning potential

Valerij A. Shklovskij

*Institute of Theoretical Physics, National Science Center–Kharkov Institute of Physics and Technology, 61108 Kharkov, Ukraine
and Department of Physics, Kharkov National University, 61077 Kharkov, Ukraine*

Oleksandr V. Dobrovolskiy

Department of Physics, Kharkov National University, 61077 Kharkov, Ukraine

(Received 21 July 2008; published 29 September 2008)

The Langevin equation for a two-dimensional (2D) nonlinear guided vortex motion in a tilted cosine pinning potential in the presence of an ac is *exactly* solved in terms of a *matrix* continued fraction at arbitrary value of the Hall effect. The influence of an ac of arbitrary amplitude and frequency on the dc and ac magnetoresistivity tensors is analyzed. The ac density and frequency dependence of the overall shape and the number and position of the Shapiro steps on the anisotropic current-voltage characteristics are considered. The influence of a subcritical or overcritical dc on the time-dependent stationary ac longitudinal and transverse resistive vortex responses (on the frequency of an ac drive Ω) in terms of the nonlinear impedance tensor \hat{Z} and the nonlinear ac response at Ω harmonics are studied. Analytical formulas for 2D temperature-dependent *linear* impedance tensor \hat{Z}_L in the presence of a dc which depend on the angle α between the current-density vector and the guiding direction of the washboard planar pinning potential are derived and analyzed. Influence of α anisotropy and the Hall effect on the nonlinear power absorption by vortices is discussed.

DOI: 10.1103/PhysRevB.78.104526

PACS number(s): 74.25.Fy, 74.25.Sv, 74.25.Qt

I. INTRODUCTION

It is well known that the mixed-state resistive properties of type-II superconductors are determined by the dynamics of vortices which in the presence of pinning sites may be described as a motion of vortices in some pinning potential.¹ In the simplest case this pinning potential is assumed to be periodic in one dimension. Temperature-dependent dc uniaxial pinning anisotropy, provoked by such washboard planar pinning potential (PPP), recently has been extensively studied both theoretically^{2–4} and experimentally.^{5–9} Two main reasons stimulated these studies. First, in some high- T_c superconductors (HTSCs) twins can easily be formed during the crystal growth.^{5–7} Second, in layered HTSCs the system of interlayers between parallel *ab* planes can be considered as a set of unidirectional planar defects which provoke the intrinsic pinning of vortices.¹

As the pinning force in a PPP is directed perpendicular to the washboard channels of the PPP,¹ the vortices generally tend to move along these channels. Such a *guided* motion of vortices in the presence of the Hall effect produces anisotropic transport behavior for which even (+) and odd (–) (with respect to the magnetic-field reversal) longitudinal (\parallel) and transverse (\perp) dc nonlinear magnetoresistivities $\rho_{\parallel,\perp}^{\pm}$ depend substantially on the angle α between the dc density vector \mathbf{j} and the direction of the PPP channels (“guiding direction”). The dc nonlinear guiding problem was exactly solved recently for the washboard PPP within the framework of the two-dimensional (2D) single-vortex stochastic model of anisotropic pinning based on the Fokker-Planck equation, and rather simple formulas were derived for the dc magnetoresistivities $\rho_{\parallel,\perp}^{\pm}$.^{2,3}

On the other hand, the high-frequency and microwave *impedance* measurements of a mixed state can also give in-

formation about the flux pinning mechanisms and the vortex dynamics. One of the most popular experimental methods for the investigation of the vortex dynamics in type-II superconductors is the measurement of the complex ac response in the radiofrequency and microwave ranges. When the Lorentz force acting on the vortices is alternating, then due to the pinning the ac resistive response acquires an imaginary (out-of-phase) component. Due to this reason measurements of the complex ac response versus frequency ω can give important information on the pinning forces.

The very early model of Gittleman and Rosenblum¹⁰ (GR) considers oscillations of damped vortex in a harmonic pinning potential. GR measured the power absorption of the vortices in PbIn and NbTa films over a wide range of frequencies ω and successfully analyzed their data with the simple equation

$$\eta\dot{x} + k_p x = F_L, \quad (1)$$

where x is the vortex displacement, η is the vortex viscosity, k_p is the pinning constant, and F_L is the Lorentz force. From Eq. (1) it follows that the complex vortex resistivity ρ_v is

$$(\rho_v/\rho_f) = i(\omega/\omega_p)/[1 + i(\omega/\omega_p)], \quad (2)$$

where ρ_f is the flux-flow resistivity and $\omega_p \equiv k_p/\eta$ is the depinning frequency. As follows from Eqs. (1) and (2), pinning forces dominate at low frequencies ($\omega \ll \omega_p$) where ρ_v is nondissipative, whereas at high frequencies ($\omega \gg \omega_p$) frictional forces dominate and the vortex resistivity is dissipative.

The experimental success of this very simple model stimulated the attempts to use it for the interpretation of the data taken in HTSCs, where the effects of thermal agitation are especially important due to their low pinning activation

energies and the high temperatures of the superconducting state. As the GR model was developed for zero temperature and cannot account for the thermally activated flux flow and creep, which are very pronounced in HTSCs, there was a need for a more general model for the ac vortex dissipation at different temperatures and frequencies.

In order to fulfill this aim the vortex equation of motion [Eq. (1)] was supplemented with Langevin force which was assumed to be Gaussian white noise with zero mean, and the cosine periodic pinning potential was used^{11–13} for taking into account the possibility of vortex hopping between different potential wells. In the limit of small ac (i.e., for a *nontilted* cosine pinning potential), this new equation of motion was approximately solved by a continued-fraction expansion^{11–13} using the analogy between a pinned vortex and a Brownian particle motion in a periodic potential. As a result, the complex resistivity ρ_v which generalizes GR equation (2) has the form [see Eq. (8) of Ref. 11]

$$(\rho_v/\rho_f) = [i(\omega/\omega_0) + \nu_{00}]/[1 + i(\omega/\omega_0)], \quad (3)$$

where ν_{00} is a creep factor that grows monotonically with temperature, increasing from $\nu_{00}=0$ (no flux creep) to $\nu_{00}=1$ (flux-flow regime), and ω_0 is a characteristic frequency (nonmonotonic in temperature) which, in absence of creep, corresponds to the depinning frequency ω_p . If the frequency ω is swept across the temperature-dependent frequency ω_0 , the observed $\text{Re } \rho_v$ increases from a low-frequency value to the flux-flow value ρ_f , while $\text{Im } \rho_v$ exhibits a maximum at ω_0 . Thus, we can summarize that the temperature-dependent ac-driven vortex motion problem has been *exactly* solved so far only for the one-dimensional (1D) *nontilted* cosine pinning potential at a small oscillation amplitude of the vortices.

At the same time, the examination of a *strong* ac drive (which is interesting both for theory and for different high-frequency or microwave applications) evidently requires one to consider strongly *tilted* pinning potential. Actually, if at low temperatures and relatively high frequencies in *nontilted* pinning potential each pinned vortex will be confined to its pinning potential well during the ac period, in the case of strong ac+dc driving current the *running* states of the vortex may appear when it can visit several potential wells during the ac period.

The aim of this work is to suggest a theoretical approach to the study of temperature-dependent *nonlinear* ac-driven pinning-mediated vortex dynamics based on an *exact* solution (in terms of a *matrix* continued fraction) of the same equation of vortex motion, as was discussed by Coffey and Clem¹¹ (CC) in a seminal paper [see Eq. (4), which has an additional Hall term]. This approach substantially generalizes CC's results because the 2D Langevin equation for the nonlinear guided motion in a *tilted* cosine PPP in the presence of a strong ac at arbitrary value of the Hall effect has been exactly solved. For this exact solution we used the matrix continued-fraction technique earlier suggested and later extensively employed for calculation of 1D nonlinear (ac+dc)-driven response of overdamped Josephson junction with noise in Refs. 14 and 15.

As a result, two groups of findings were obtained. First, for the previously solved 2D dc problem in Refs. 2 and 3 the

influence of an ac on the overall shape and appearance of the Shapiro steps on the anisotropic dc $\rho_{\parallel,\perp}^{\pm}$ current-voltage characteristics (CVCs) was calculated and analyzed. Second, for the ac at a frequency ω plus dc bias the 2D nonlinear time-dependent stationary $\rho_{\parallel,\perp}^{\text{ac}\pm}$ ac response on the frequency ω in terms of nonlinear impedance tensor \hat{Z} and a nonlinear ac response at ω harmonics was studied.

The organization of the paper is as follows: In Sec. II we introduce the model and the basic quantities of interest, namely, the average two-dimensional electric field and the Fourier amplitudes for the averaged moments $\langle r^m \rangle$. In Sec. III we present the solution of the recurrence equations for the Fourier amplitudes in terms of matrix continued fraction and introduce the main anisotropic nonlinear component of our theory—the average pinning force, divided into three parts. In Sec. IV we discuss the ω -dependent dc magnetoresistivity response with different (from Secs. IV A and IV E) aspects of this problem. Sections V A and V H present different problems related to nonlinear anisotropic stationary ac response. In Sec. VI we conclude with a general discussion of our results.

II. FORMULATION OF THE PROBLEM

The Langevin equation for a vortex moving with velocity \mathbf{v} in a magnetic field $\mathbf{B}=\mathbf{n}B$ ($B\equiv|\mathbf{B}|$, $\mathbf{n}=\mathbf{n}z$, \mathbf{z} is the unit vector in the z direction, and $n=\pm 1$) has the form

$$\eta\mathbf{v} + n\alpha_H\mathbf{v} \times \mathbf{z} = \mathbf{F}_L + \mathbf{F}_p + \mathbf{F}_{\text{th}}, \quad (4)$$

where $\mathbf{F}_L=n(\Phi_0/c)\mathbf{j} \times \mathbf{z}$ is the Lorentz force (Φ_0 is the magnetic flux quantum and c is the speed of light); $\mathbf{j}=\mathbf{j}(t)=\mathbf{j}^{\text{dc}} + \mathbf{j}^{\text{ac}} \cos \omega t$, where \mathbf{j}^{dc} and \mathbf{j}^{ac} are the dc and ac density amplitudes and ω is the angular frequency; $\mathbf{F}_p=-\nabla U_p(x)$ is the anisotropic pinning force [$U_p(x)$ is the washboard planar pinning potential]; \mathbf{F}_{th} is the thermal fluctuation force; η is the vortex viscosity; and α_H is the Hall constant. We assume that the fluctuational force $\mathbf{F}_{\text{th}}(t)$ is represented by a Gaussian white noise, whose stochastic properties are assigned by the relation

$$\langle F_{\text{th},i}(t) \rangle = 0, \quad \langle F_{\text{th},i}(t) F_{\text{th},j}(t') \rangle = 2T\eta\delta_{ij}\delta(t-t'), \quad (5)$$

where T is the temperature in energy units, $\langle \dots \rangle$ means the statistical average, and $F_{\text{th},i}(t)$ with $i=x$ or $i=y$ is the i component of $\mathbf{F}_{\text{th}}(t)$.

The formal statistical average of Eq. (4) is

$$\eta\langle \mathbf{v} \rangle + n\alpha_H\langle \mathbf{v} \rangle \times \mathbf{z} = \mathbf{F}_L + \langle \mathbf{F}_p \rangle. \quad (6)$$

Though $\langle \mathbf{F}_{\text{th}} \rangle$ disappears because of the stochastic property in Eq. (5), effects of the thermal fluctuation are implicit in the term $\langle \mathbf{F}_p \rangle$ (see below).

Since the anisotropic pinning potential is assumed to depend only on the x coordinate and is assumed to be periodic [$U_p(x)=U_p(x+a)$, where a is the period], the pinning force is always directed along the anisotropy axis x (with unity vector \mathbf{x} ; see Fig. 1) so that it has no component along the y axis ($F_{py}=-dU_p/dy=0$). Thus, Eq. (4) reduces to the equations

$$\begin{aligned} v_x + \delta v_y &= (F_{Lx} + F_{px} + F_x)/\eta, \\ v_y - \delta v_x &= (F_{Ly} + F_y)/\eta, \end{aligned} \quad (7)$$

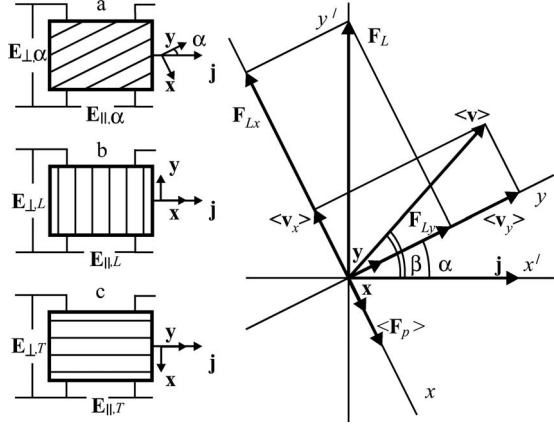


FIG. 1. System of coordinates xy (with the unit vectors \mathbf{x} and \mathbf{y}) associated with the PPP washboard channels and the system of coordinates $x'y'$ associated with the direction of the current-density vector \mathbf{j} . α is the angle between the channels of the PPP and \mathbf{j} , and β is the angle between the average velocity vector of the vortices $\langle \mathbf{v} \rangle$ and \mathbf{j} . \mathbf{F}_L is the Lorentz force, $\langle \mathbf{F}_p \rangle$ is the average pinning force, and \mathbf{F}_{Lx} is the average effective motive force for a vortex. Here for simplicity we assume $\epsilon=0$. The schematic sample configuration for three cases with different values of angle α (inset): general case, $\alpha \neq 0, \pi/2$ (a); longitudinal L geometry, $\alpha = \pi/2$, $\mathbf{j} \perp \mathbf{y}$ (b); and transverse T geometry, $\alpha = 0$, $\mathbf{j} \parallel \mathbf{x}$ (c). In all cases \mathbf{E}_\perp and \mathbf{E}_\parallel are transverse and longitudinal (with respect to the \mathbf{j} direction) electric-field components.

where $\delta \equiv n\epsilon$ and $\epsilon \equiv \alpha_H / \eta$, and we omitted the index “th” for simplicity. Equation (7) can be rewritten for the subsequent analysis in the following form:

$$v_x \equiv \dot{x} = (\tilde{F}_{Lx} + F_{px} + \tilde{F}_x) / \eta D, \quad (8)$$

$$v_y \equiv \dot{y} = (\tilde{F}_{Ly} + \tilde{F}_y + \delta F_{px}) / \eta D,$$

where $\tilde{F}_{Lx} \equiv F_{Lx} - \delta F_{Ly}$, $\tilde{F}_{Ly} \equiv F_{Ly} + \delta F_{Lx}$, $\tilde{F}_x \equiv F_x - \delta F_y$, $\tilde{F}_y \equiv F_y + \delta F_x$, $D \equiv 1 + \delta^2$, and $\langle \tilde{F}_i(t) \tilde{F}_j(t') \rangle = 2T\eta D \delta_{ij} \delta(t-t')$.

Our aim now is to obtain from Eq. (8) a rigorous and explicit expression of $\langle v_x \rangle$ and $\langle v_y \rangle$ in which effects of the pinning and the thermal fluctuation are considered. We assume, as usual,^{2,11-13} a periodic pinning potential of the form $U_p(x) = (U_p/2)(1 - \cos kx)$, where $k = 2\pi/a$. As $F_{px} = -F_p \sin kx$, where $F_p \equiv U_p k/2$, the first line of Eq. (8) has the form

$$\hat{\tau}(dx/dt) + \sin x = \hat{F}_{Lx} + \hat{F}_x. \quad (9)$$

Here $x = kx$ is the dimensionless vortex coordinate, $\hat{\tau} \equiv \eta D / kF_p$ is the relaxation time, $\hat{F}_{Lx} = \tilde{F}_{Lx} / F_p$ is the dimensionless generalized moving force in the x direction, $\hat{F}_x = \tilde{F}_x / F_p$, and $\langle \hat{F}_x(t) \hat{F}_x(t') \rangle = \tau \delta(t-t')$, where $\tau \equiv 2\hat{\tau} / g$ and $g = U_p / 2T$ is the dimensionless inverse temperature.

Making the transformation $x(t) \rightarrow r^m(t) = e^{-imx(t)}$ in Eq. (9), one obtains a stochastic differential equation with a multiplicative noise term, the averaging of which yields a system of differential-recurrence relations for the moments $\langle r^m \rangle = \langle e^{-imx} \rangle$ (as described in detail in Ref. 14), viz.,

$$\hat{\tau} d\langle r^m \rangle(t) / dt + [m^2/g + im\hat{F}_{Lx}] \langle r^m \rangle(t) = (m/2) [\langle r^{m-1} \rangle(t) - \langle r^{m+1} \rangle(t)]. \quad (10)$$

The main quantity of physical interest in our problem is the average electric field, induced by the moving vortex system, which is given by

$$\langle \mathbf{E} \rangle = (n/c) \mathbf{B} \times \langle \mathbf{v} \rangle = n(B/c) (-\langle v_y \rangle \mathbf{x} + \langle v_x \rangle \mathbf{y}), \quad (11)$$

where \mathbf{x} and \mathbf{y} are the unit vectors in the x and y directions, respectively.

As follows from Eq. (8)

$$\langle v_y \rangle = F_{Ly} / \eta + \delta \langle v_x \rangle, \quad (12)$$

and so for determination of $\langle \mathbf{E} \rangle$ from Eq. (11) it is sufficient to calculate the $\langle v_x \rangle$ from Eq. (9). This calculation gives

$$\langle v_x \rangle(t) = \frac{\Phi_0 j_c}{c \eta D} [j^{dc} + j^{ac} \cos \omega t - \langle \sin x \rangle(t)], \quad (13)$$

where

$$\langle \sin x \rangle(t) = \frac{i}{2} [\langle r \rangle(t) - \langle r^{-1} \rangle(t)]. \quad (14)$$

In Eq. (10) $j^{dc} \equiv n(j_y^{dc} + \delta j_x^{dc}) / j_c$, $j^{ac} \equiv n(j_y^{ac} + \delta j_x^{ac}) / j_c$, and $j_c \equiv cF_p / \Phi_0$.

Since we are only concerned with the stationary ac response, which is independent of the initial condition, one needs to calculate the solution of Eq. (10) corresponding to the stationary case. To accomplish this, one may seek all the $\langle r^m \rangle(t)$ in the form

$$\langle r^m \rangle(t) = \sum_{k=-\infty}^{\infty} F_k^m(\omega) e^{ik\omega t}. \quad (15)$$

On substituting Eq. (15) into Eq. (10), we obtain recurrence equations for the Fourier amplitudes $F_k^m(\omega)$, i.e.,

$$F_k^{m+1}(\omega) - F_k^{m-1}(\omega) + iz_{m,k}(\omega) F_k^m(\omega) + ij^{ac} [F_{k-1}^m(\omega) + F_{k+1}^m(\omega)] = 0, \quad (16)$$

where

$$z_{m,k}(\omega) = 2(j^{dc} + \omega \hat{\tau} k / m - im/g). \quad (17)$$

III. SOLUTION OF THE PROBLEM IN TERMS OF MATRIX CONTINUED FRACTIONS

Scalar five-term recurrence equation (16) can be transformed into the two uncoupled matrix three-term recurrence relations

$$\mathbf{Q}_m(\omega) \mathbf{C}_m(\omega) + \mathbf{C}_{m+1}(\omega) = \mathbf{C}_{m-1}(\omega) \quad (m = 1, 2, \dots) \quad (18)$$

and

$$-\mathbf{Q}_m^*(-\omega) \mathbf{C}_{-m}(\omega) + \mathbf{C}_{-m+1}(\omega) = \mathbf{C}_{-m-1}(\omega) \quad (m = 1, 2, \dots), \quad (19)$$

where \mathbf{Q}_m is a tridiagonal infinite matrix given by

$$\mathbf{Q}_m(\omega) = i \begin{pmatrix} \ddots & \vdots & \vdots & \vdots & \ddots \\ \cdots & z_{m,-2}(\omega) & j^{\text{ac}} & 0 & \cdots \\ \cdots & j^{\text{ac}} & z_{m,-1}(\omega) & j^{\text{ac}} & 0 \\ \cdots & 0 & j^{\text{ac}} & z_{m,0}(\omega) & j^{\text{ac}} \\ \cdots & \cdots & 0 & j^{\text{ac}} & z_{m,1}(\omega) \\ \cdots & \cdots & \cdots & 0 & j^{\text{ac}} \\ \ddots & \vdots & \vdots & \vdots & \ddots \end{pmatrix} \quad (20)$$

(the asterisk denotes the complex conjugate), and the infinite column vectors $\mathbf{C}_m(\omega)$ are defined as

$$\mathbf{C}_m(\omega) = \begin{pmatrix} \vdots \\ F_{-2}^m(\omega) \\ F_{-1}^m(\omega) \\ F_0^m(\omega) \\ F_1^m(\omega) \\ F_2^m(\omega) \\ \vdots \end{pmatrix} \quad \text{for } m = \pm 1, \pm 2, \dots, \quad (21)$$

$$\mathbf{C}_0 = \begin{pmatrix} \vdots \\ 0 \\ 0 \\ 1 \\ 0 \\ 0 \\ \vdots \end{pmatrix} \quad \text{for } m = 0.$$

Thus, in order to calculate $\langle \sin x \rangle(t)$ in Eq. (14), we need to evaluate $\mathbf{C}_1(\omega)$ and $\mathbf{C}_{-1}(\omega)$, which contain all the Fourier amplitudes of $\langle r \rangle(t)$ and $\langle r^{-1} \rangle(t)$. Equation (18) can be solved for \mathbf{C}_1 in terms of matrix continued fractions,¹⁴ viz.,

$$\mathbf{C}_1(\omega) = \frac{\mathbf{I}}{\mathbf{Q}_1(\omega) + \frac{\mathbf{I}}{\mathbf{Q}_2(\omega) + \frac{\mathbf{I}}{\mathbf{Q}_3(\omega) + \cdots}}} \mathbf{C}_0, \quad (22)$$

where the fraction lines designate the matrix inversions and \mathbf{I} is the identity matrix of infinite dimension. Having determined $\mathbf{C}_1(\omega)$, it is not necessary to solve Eq. (19), as all the components of the column vector $\mathbf{C}_{-1}(\omega)$ can be obtained from Eq. (22) on noting that

$$F_0^1(\omega) = F_0^{-1*}(\omega) \quad \text{and} \quad F_k^{-1}(\omega) = F_{-k}^{1*}(\omega). \quad (23)$$

Following the solutions of Eq. (22) and using relation (23), we can find the dimensionless average pinning force $\langle F_{px} \rangle(t)$ [see Eqs. (6)–(9), (14), and (15)], which is the main anisotropic nonlinear (due to a dependence on the ac and dc input) component of the theory under discussion,

$$\langle \hat{F}_{px} \rangle(t) = -\langle \sin x \rangle(t) = \sum_{k=0}^{\infty} \text{Im}(\psi_k e^{ik\omega t}), \quad (24)$$

where $\psi_0 \equiv F_0^1(\omega)$ and for $k \geq 1$ we have $\psi_k \equiv F_k^1(\omega) - F_k^{-1}(\omega)$.

In fact, Eq. (24) is the expansion of the stationary time-dependent (and independent of the initial conditions) average pinning force $\langle \hat{F}_{px} \rangle(t)$ into three parts,

$$\langle \hat{F}_{px} \rangle(t) = \langle \hat{F}_{px} \rangle_0^\omega + \langle \hat{F}_{px} \rangle_{t1} + \langle \hat{F}_{px} \rangle_t^{k>1}. \quad (25)$$

In Eq. (25) $\langle \hat{F}_{px} \rangle_0^\omega \equiv -\langle \sin x \rangle_0^\omega = \text{Im} \psi_0$ is the time-independent (but frequency-dependent) *static* average pinning force, which will be used for the derivation of the dc magnetoresistivity tensor $\hat{\rho}_0^\omega$. $\langle \hat{F}_{px} \rangle_{t1} \equiv -\langle \sin x \rangle_{t1} = \text{Im}(\psi_1 e^{i\omega t})$ is the time-dependent *dynamic* average pinning force with a frequency ω of the ac input, which is responsible for the nonlinear impedance $Z_1(\omega)$. $\langle \hat{F}_{px} \rangle_t^{k>1} \equiv -\langle \sin x \rangle_t^{k>1} = \text{Im}(\psi_k e^{ik\omega t})$ describes a contribution of the *harmonics* with $k > 1$ into the dynamic average pinning force.

IV. ω -DEPENDENT dc MAGNETORESISTIVITY RESPONSE

A. Nonlinear dc resistivity and conductivity tensors

In order to proceed with these calculations we first express [see Eq. (11)] the time-independent part of $\langle E_y \rangle(t) = (nB/c) \langle v_x \rangle(t)$ as

$$\begin{aligned} \langle E_y \rangle_0^\omega &= (nB/c) \langle v_x \rangle_0^\omega \equiv (n\rho_f/D)(j^{\text{dc}} - \langle \sin x \rangle_0^\omega) \\ &= (\rho_f/D) \nu_0^\omega (j_y^{\text{dc}} + \delta_j^{\text{dc}}), \end{aligned} \quad (26)$$

where

$$\nu_0^\omega \equiv 1 - \langle \sin x \rangle_0^\omega / j^{\text{dc}} = 1 + \langle \hat{F}_{px} \rangle_0^\omega / j^{\text{dc}}. \quad (27)$$

In Eq. (26) $\rho_f \equiv B\Phi_0 / \eta c^2$ is the flux-flow resistivity and the ν_0^ω can be considered as the $(\omega, j^{\text{dc}}, j^{\text{ac}}, T)$ -dependent effective mobility of the vortex under the influence of the dimensionless generalized moving force $\hat{F}_{Lx}^{\text{dc}} = j^{\text{dc}}$ in the x direction. In the absence of the ac [see Eq. (35)] the ν_0^ω coincides with the probability of vortex hopping over the pinning potential barrier.³

From Eq. (27) follows *another* physical interpretation of the ν_0^ω function, which has a close relationship with the average pinning force $\langle \hat{F}_{px} \rangle_0^\omega$ acting on the vortex. Actually, it is evident from Eq. (27) that the $\langle \hat{F}_{px} \rangle_0^\omega$ is connected to the ν_0^ω function in a simple way,

$$\langle \hat{F}_{px} \rangle_0^\omega = -\hat{F}_{Lx}^{\text{dc}}(1 - \nu_0^\omega). \quad (28)$$

Then it is easy to show that

$$\langle E_x \rangle_0^\omega = (\rho_f/D) \{ j_x^{\text{dc}} [1 + \delta^2(1 - \nu_0^\omega)] - \delta j_y^{\text{dc}} \}. \quad (29)$$

From Eqs. (26) and (29) we find the $(\omega, j^{\text{dc}}, j^{\text{ac}}, T)$ -dependent magnetoresistivity tensor for the dc-measured nonlinear law $\langle \mathbf{E}_0^\omega(\omega) \rangle = \hat{\rho}_0^\omega \mathbf{j}^{\text{dc}}$ as

$$\hat{\rho}_0^\omega = \begin{pmatrix} \rho_{xx}^{\text{dc}} & \rho_{xy}^{\text{dc}} \\ \rho_{yx}^{\text{dc}} & \rho_{yy}^{\text{dc}} \end{pmatrix} = \frac{\rho_f}{D} \begin{pmatrix} 1 + \delta^2(1 - \nu_0^\omega) & -\delta\nu_0^\omega \\ \delta\nu_0^\omega & \nu_0^\omega \end{pmatrix}. \quad (30)$$

The dc conductivity tensor $\hat{\sigma}_0^\omega$, which is the inverse tensor to $\hat{\rho}_0^\omega$, has the form

$$\hat{\sigma}_0^\omega = \begin{pmatrix} \sigma_{xx}^{\text{dc}} & \sigma_{xy}^{\text{dc}} \\ \sigma_{yx}^{\text{dc}} & \sigma_{yy}^{\text{dc}} \end{pmatrix} = \frac{1}{\rho_f} \begin{pmatrix} 1 & \delta \\ -\delta & (D/\nu_0^\omega) - \delta^2 \end{pmatrix}. \quad (31)$$

We see from Eqs. (30) and (31) that the off-diagonal components of the $\hat{\rho}_0^\omega$ and $\hat{\sigma}_0^\omega$ tensors satisfy the Onsager relation ($\rho_{xy} = -\rho_{yx}$ in the general nonlinear case and $\sigma_{xy} = -\sigma_{yx}$). All the components of the $\hat{\rho}_0^\omega$ tensor and one of the diagonal components of the $\hat{\sigma}_0^\omega$ tensor are functions of the current densities j^{dc} and j^{ac} and ω through the external force \hat{F}_{Lx} , the temperature T , the angle α , and the dimensionless Hall parameter $\delta = n\epsilon$. It is important, however, to stress that the off-diagonal components of the $\hat{\sigma}_0^\omega$ are not influenced by the presence of the pinning potential barriers.

In conclusion of this subsection let us consider the limiting case $j^{\text{ac}} = 0$, i.e., we should derive a *static* CVC. In this case we have from Eq. (10) that

$$(m + igj^{\text{dc}})\langle r^m \rangle_0 = (g/2)(\langle r^{m-1} \rangle_0 - \langle r^{m+1} \rangle_0), \quad (32)$$

where the subscript “0” denotes the statistical average in the absence of the ac. In order to solve Eq. (32) we introduce, following the calculation of Risken,¹⁶ the quantity $S_m = \langle r^m \rangle_0 / \langle r^{m-1} \rangle_0$, which satisfies the equation

$$(m + igj^{\text{dc}})S_m = (g/2)(1 - S_m S_{m+1}). \quad (33)$$

The solution of Eq. (33) (see details in Ref. 14) can be expressed in terms of the modified Bessel functions $I_\nu(z)$ of the first kind of order ν (where ν may be a complex number¹⁷) as

$$S_m = I_{m+\mu}(g)/I_{m-\mu}(g), \quad (34)$$

where $\mu \equiv igj^{\text{dc}}$. Taking into account Eqs. (27) and (34) and the relation $S_1 = \langle r \rangle_0 = \langle \cos x \rangle_0 - i\langle \sin x \rangle_0$, we conclude that $\langle \hat{F}_{px} \rangle_0 = \text{Im} S_1 = \text{Im}[I_{1+\mu}(g)/I_{\mu}(g)]$ and

$$\nu_0 \equiv \nu_0^\omega(j^{\text{ac}} = 0, \omega = 0) = 1 + \text{Im} S_1/j^{\text{dc}} = 1 + \text{Im}[I_{1+\mu}(g)/I_{\mu}(g)]/j^{\text{dc}}. \quad (35)$$

Note that Eq. (35) gives a simpler analytical expression for the ν_0 function which was presented in Ref. 2 on the basis of a Fokker-Planck approach, namely,

$$\nu_0^{-1}(F) = \frac{F}{1 - e^{-F}} \int_0^1 du e^{-Fu} I_0(2g \sin \pi u), \quad (36)$$

with $F \equiv 2\pi g j^{\text{dc}}$, where $g = U_p/2T$ is the dimensionless inverse temperature. In Fig. 2 we plotted $\nu_0^\omega(\xi^d, \xi^a)$ graphs at $g = 30$, which demonstrate in the limit of $\xi^a = 0$ the ξ^d dependence for the probability of vortex hopping over the tilted cosine pinning potential barrier. Here ξ^d and ξ^a are the dimensionless dc and maximal ac density magnitudes (in j_c units), respectively ($\xi^d \equiv j^d/j_c$, $\xi^a \equiv j^a/j_c$).

B. Longitudinal and transverse dc resistivities

The experimentally measurable resistive dc responses refer to coordinate system tied to the dc (see Fig. 1). The

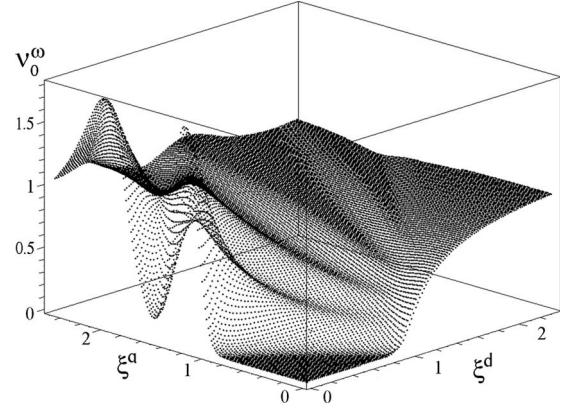


FIG. 2. The dimensionless function $\nu_0^\omega(\xi^d, \xi^a)$ numerically obtained from Eq. (27) at $g = 30$ and $\omega\hat{\tau} = 0.2$.

longitudinal and transverse (with respect to the dc direction) components of the electric field, $E_{\parallel}^{\text{dc}}$ and E_{\perp}^{dc} , are related to $E_x^{\text{dc}} \equiv \langle E_x \rangle_0^\omega$ and $E_y^{\text{dc}} \equiv \langle E_y \rangle_0^\omega$ by the simple expressions

$$E_{\parallel}^{\text{dc}} = E_x^{\text{dc}} \sin \alpha + E_y^{\text{dc}} \cos \alpha,$$

$$E_{\perp}^{\text{dc}} = -E_x^{\text{dc}} \cos \alpha + E_y^{\text{dc}} \sin \alpha. \quad (37)$$

Then according to Eq. (37), the expressions for the experimentally observable longitudinal and transverse (with respect to the \mathbf{j}^{dc} direction) magnetoresistivities $\rho_{\parallel}^{\text{dc}} = E_{\parallel}^{\text{dc}}/j^d$ and $\rho_{\perp}^{\text{dc}} = E_{\perp}^{\text{dc}}/j^d$ [where j^d is the dc density $(j^d)^2 = (j_x^{\text{dc}})^2 + (j_y^{\text{dc}})^2$] have the form

$$\rho_{\parallel}^{\text{dc}} = \rho_{xx}^{\text{dc}} \sin^2 \alpha + \rho_{yy}^{\text{dc}} \cos^2 \alpha,$$

$$\rho_{\perp}^{\text{dc}} = \rho_{yx}^{\text{dc}} \sin^2 \alpha - \rho_{xy}^{\text{dc}} \cos^2 \alpha + (\rho_{yy}^{\text{dc}} - \rho_{xx}^{\text{dc}}) \sin \alpha \cos \alpha. \quad (38)$$

Note, however, that the magnitudes of the $\rho_{\parallel}^{\text{dc}}$ and ρ_{\perp}^{dc} , given by Eq. (38) and applied to the dc responses, in general, depend on the direction of the external magnetic field \mathbf{B} along the z axis due to the $\delta = n\epsilon$ dependence of the ν_0^ω function [see Eq. (27)]. In order to consider only n -independent magnitudes of the $\rho_{\parallel}^{\text{dc}}$ and ρ_{\perp}^{dc} responses, we should introduce the even (+) and odd (−) magnetoresistivities with respect to magnetic-field reversal ($\rho^{\text{dc}\pm}(n) \equiv [\rho^{\text{dc}}(n) \pm \rho^{\text{dc}}(-n)]/2$) for longitudinal and transverse dimensional magnetoresistivities, which in view of Eq. (38) have the forms

$$\rho_{\parallel}^{\text{dc}\pm} = (\rho_f/D)[(\cos^2 \alpha - \delta^2 \sin^2 \alpha)\nu_0^{\omega\pm} + D(1 \pm 1)\sin^2 \alpha/2], \quad (39)$$

$$\rho_{\perp}^{\text{dc}\pm} = (\rho_f/D)[D\nu_0^{\omega\pm} \sin \alpha \cos \alpha + \delta\nu_0^{\omega\mp} - D(1 \pm 1)\sin \alpha \cos \alpha/2], \quad (40)$$

where $\nu_0^{\omega\pm}(n) = [\nu_0^\omega(n) \pm \nu_0^\omega(-n)]/2$ are the even and odd components relative to the magnetic-field inversion of the function $\nu_0^\omega(n)$. In the $E_{\parallel,\perp}^{\text{dc}\pm}(j)$ dependences, which follow from Eqs. (39) and (40), the nonlinear and linear (nonzero only for $\rho_{\parallel}^{\text{dc}+}$ and $\rho_{\perp}^{\text{dc}+}$) terms separate out in a natural way. The physical reason for the appearance of linear terms is that in the model under consideration for $\alpha \neq 0$ there is always

the flux-flow regime of vortex motion along the channels of the PPP. It follows from Eqs. (39) and (40) that for $\alpha \neq 0, \pi/2$ the observed resistive response contains not only the ordinary longitudinal $\rho_{\parallel}^{\text{dc}+}(\alpha)$ and transverse $\rho_{\perp}^{\text{dc}-}(\alpha)$ magnetoresistivities, but also (as in the absence of ac; see Ref. 3) two new components, induced by the pinning anisotropy: an *even transverse* $\rho_{\perp}^{\text{dc}+}(\alpha)$ and the *odd longitudinal* component $\rho_{\parallel}^{\text{dc}-}(\alpha)$.

In the absence of ac [$v_0 \equiv v_0^{\omega}(\xi^{\alpha}=0, \omega=0)$] the physical origin of the $\rho_{\perp}^{\text{dc}+}(\alpha)$ (which is independent of ϵ at $\epsilon \ll 1$) is related to the guided vortex motion along the channels of the washboard pinning potential in the thermoactivated flux-flow (TAFF) regime. On the other hand, the $\rho_{\parallel}^{\text{dc}-}(\alpha)$ component is proportional to the odd component v_0^- , which is zero at $\epsilon = 0$ and has a maximum in the region of the nonlinear transition from the TAFF to the FF regime at $\epsilon \neq 0$ (see Figs. 6 and 7 of Ref. 3). The (j^{dc}, g) dependence of the odd transverse (Hall) resistivity has contributions both from the even v_0^+ and from the odd v_0^- components of the $v_0(j^{\text{dc}}, g)$ function. Their relative magnitudes are determined by the angle α and the dimensionless Hall constant ϵ . Note that as the odd longitudinal $\rho_{\parallel}^{\text{dc}-}$ and odd transverse $\rho_{\perp}^{\text{dc}-}$ magnetoresistivities arise by virtue of the Hall effect, their characteristic scale is proportional to $\epsilon \ll 1$.

C. dc response in LT geometries

In order to analyze the simplest forms of the $\rho_{\parallel, \perp}^{\text{dc}\pm}$ equations given by formulas (39) and (40), we introduce the L and T geometries (see Fig. 1), in which $\mathbf{j} \parallel \mathbf{x}$ (i.e., $\alpha = \pi/2$) and $\mathbf{j} \perp \mathbf{x}$ (i.e., $\alpha = 0$ and $\mathbf{j} \parallel \mathbf{y}$), respectively. It follows from Eqs. (39) and (40) that the longitudinal $\rho_{\parallel}^{\text{dc}-}$ and transverse $\rho_{\perp}^{\text{dc}+}$ resistivities for a superconductor with uniaxial pinning anisotropy in LT geometries vanish (i.e., $\rho_{\parallel}^{\text{dc}-} = \rho_{\perp}^{\text{dc}+} = 0$). We obtain

$$\rho_{\parallel, T}^{\text{dc}+} = v_{0, T}^{\omega} / D, \quad \rho_{\perp, T}^{\text{dc}-} = n \epsilon v_{0, T}^{\omega} / D, \quad (41)$$

$$\rho_{\parallel, L}^{\text{dc}+} = 1 - \epsilon^2 v_{0, L}^{\omega} / D, \quad \rho_{\perp, L}^{\text{dc}-} = n \epsilon v_{0, L}^{\omega} / D. \quad (42)$$

Here $v_{0, T}^{\omega} \equiv v_0^{\omega}(j_T^{\text{dc}}, j_T^{\text{ac}}, \omega, g)$, $v_{0, L}^{\omega} \equiv v_0^{\omega}(j_L^{\text{dc}}, j_L^{\text{ac}}, \omega, g)$, $j_T^{\text{dc}} \equiv n \xi^d$, $j_T^{\text{ac}} \equiv n \xi^a$, $j_L^{\text{dc}} \equiv \epsilon \xi^d$, and $j_L^{\text{ac}} \equiv \epsilon \xi^a$.

If we neglect the Hall terms in Eqs. (41) and (42), then in the absence of an ac in the L geometry vortex motion takes place along the channels of the washboard PPP (the *guiding* effect), and in the T geometry transverse to the washboard channels (the *slipping* effect). In the L geometry the critical current is equal to zero since the FF regime is realized for the guided vortex motion along the PPP channels. In the T geometry, i.e., for vortex motion transverse to the channels, a pronounced nonlinear regime is realized for $g \gg 1$, the onset of which corresponds to the crossover point $j^d = j_{\text{cr}}$, and for $g \gg 1$ we have $j_{\text{cr}} = j_c$, where j_c is the critical current. The longitudinal even $\rho_{\parallel, T}^{\text{dc}+}$ and transverse odd $\rho_{\perp, T}^{\text{dc}-}$ resistivities are proportional to the even function $v_{0, T}^{\omega}(\xi^d, g)$. In the limit $j^d, g \rightarrow 0$ to within terms proportional to $\epsilon^2 \ll 1$, we have $\rho_{\parallel, T}^{\text{dc}+} = 1$ and $\rho_{\perp, T}^{\text{dc}-} = n \epsilon$. The main contribution to the $\rho_{\parallel, L}^{\text{dc}+}$, which is equal to 1 with the same accuracy, is due to the guided vortex motion along the washboard channels where the pinning is absent. The magnitude of $\rho_{\perp, L}^{\text{dc}-}$ resistivity is

described by the Magnus force $\epsilon \xi^d$, which is vanishingly small for a small Hall effect for realistically achievable currents $j^d \ll j_c / \epsilon$, and the velocity component $\langle v_x \rangle$ is suppressed; the resistivity $\rho_{\perp, L}^{\text{dc}-}$ depends mainly only on the temperature. For $g \gg 1$ the $\rho_{\perp, L}^{\text{dc}-}$ is so small that it cannot be measured ($\rho_{\perp, L}^{\text{dc}-} = 0$ in the limit $g \gg 1$ since $\epsilon \xi^d < 1$), and for $g \sim 1/2$ it approaches the value of the Hall constant ϵ (to within terms proportional to $\epsilon^2 \ll 1$).

It is worth noticing that the simple equations in Eq. (41) in the T geometry allow one to extract from the $(\xi^d, \xi^a, \omega, g)$ dependences of the measured resistivities $\rho_{\parallel, T}^{\text{dc}+}$ and $\rho_{\perp, T}^{\text{dc}-}$ the dimensionless Hall constant ϵ and the main nonlinear component of the model under discussion, $v_{0, T}^{\omega}$. The latter in the absence of ac, i.e., $v_{0, T}$, can be used for the prediction of the α -dependent $\rho_{\parallel, \perp}^{\text{dc}\pm}$ resistivities given by Eqs. (39) and (40) in the case of $\epsilon \ll 1$.

D. Guiding of vortices and the Hall effect in nonlinear dc+ac regimes

After derivation of Eqs. (39) and (40) let us proceed now to a more detailed treatment of the dc vortex dynamics and the resistive properties associated with them in the presence of an ac. For simplicity we will neglect the usually small Hall effect; i.e., we take $\epsilon = 0$. As a consequence, the nondiagonal components of the dc magnetoresistivity tensor [see Eq. (30)] vanish ($\rho_{xy}^{\text{dc}} = \rho_{yx}^{\text{dc}} = 0$). Neglecting the Hall effect, the formulas for the experimentally observed longitudinal $\rho_{\parallel}^{\text{dc}}$ and transverse ρ_{\perp}^{dc} resistivities relative to the dc+ac current can be represented as

$$\rho_{\parallel}^{\text{dc}} = \rho_f(v_0^{\omega} \cos^2 \alpha + \sin^2 \alpha), \quad (43)$$

$$\rho_{\perp}^{\text{dc}} = \rho_f[(v_0^{\omega} - 1) \sin \alpha \cos \alpha] = \rho_f j^{\text{dc}} \langle \hat{F}_{px} \rangle_0^{\omega} \sin \alpha \cos \alpha. \quad (44)$$

Therefore, as was pointed out in Ref. 3, even in the absence of ac, under certain conditions in the dc and temperature dependences of the $\rho_{\parallel}^{\text{dc}}$ and ρ_{\perp}^{dc} a pronounced nonlinearity appears in the vortex dynamics and a nonlinear guiding effect may be observed in both the inverse temperature g and the current density $j^{\text{dc}} = n \xi_y^d$. As a consequence of the even parity of v_0^{ω} in j^{dc} and $j^{\text{ac}} = n \xi_y^a$ [see Eqs. (20)–(23) and (27)] the magnetoresistivities $\rho_{\parallel}^{\text{dc}}$ and ρ_{\perp}^{dc} are even in the magnetic-field reversal, as they should be neglecting the Hall effect.

As was shown in Ref. 3, the specifics of anisotropic pinning consist of the noncoincidence of the directions of the external motive Lorentz force \mathbf{F}_L acting on the vortex and its velocity $\langle \mathbf{v} \rangle$ (for isotropic pinning $\mathbf{F}_L \parallel \langle \mathbf{v} \rangle$ if we neglect the Hall effect). The anisotropy of the pinning viscosity (which can be defined as the inverse vortex mobility $[\langle v_x \rangle_0^{\omega}]^{-1}$) along and transverse to the PPP channels leads to the result that for those values of $(j^{\text{dc}}, g, \alpha)$ for which the component of the vortex velocity perpendicular to the PPP channels, $\langle v_x \rangle_0^{\omega}$, is suppressed, a tendency appears toward a substantial prevalence of guided vortex motion along PPP channels (the *guiding* effect) over motion transverse to the channels (the *slipping* effect). In the experiment, the function

$$\cot \beta = -\frac{\rho_{\perp}^{\text{dc}}}{\rho_{\parallel}^{\text{dc}}} = \frac{1 - \nu_0^{\omega}(\xi_y^{\text{dc}}, g, \xi_y^{\text{ac}})}{\tan \alpha + \nu_0^{\omega}(\xi_y^{\text{dc}}, g, \xi_y^{\text{ac}}) \cot \alpha} \quad (45)$$

is used to describe the guiding effect, where β is the angle between the average vortex velocity vector $\langle \mathbf{v} \rangle$ and the current-density vector \mathbf{j}^{dc} (see Fig. 1). The guiding effect is stronger when the difference in directions of \mathbf{F}_L and $\langle \mathbf{v} \rangle$ is larger, i.e., the angle β is smaller. Let us consider the current and temperature dependence of $\cot \beta(\xi_y^{\text{dc}}, g, \xi_y^{\text{ac}})$ for fixed values of the angle $\alpha \neq 0, \pi/2$. In the temperature region corresponding to the TAFF regime, we have $\beta \approx \alpha$ and, consequently, at low currents guiding arises. At large currents ($\xi_y^{\text{dc}} \gg 1$), where for vortex motion transverse to the PPP channels the FF regime is set up, the vortex dynamics becomes isotropic and we have $\langle \mathbf{v} \rangle \parallel \mathbf{F}_L$ for arbitrary value of the angle α .

Let us now analyze the dc magnetoresistivity dependences $\rho_{\parallel}^{\text{dc}\pm}$ and $\rho_{\perp}^{\text{dc}\pm}$, given by Eqs. (39) and (40), with allowance for the small Hall effect. In this case, the expressions for $\rho_{\parallel, \perp}^{\text{dc}\pm}$, out to terms of order $\epsilon^2 \ll 1$, have the form

$$\begin{aligned} \rho_{\parallel}^{\text{dc}+} &= \rho_f(\nu_0^{\omega+} \cos^2 \alpha + \sin^2 \alpha), \\ \rho_{\perp}^{\text{dc}+} &= \rho_f(\nu_0^{\omega+} - 1) \sin \alpha \cos \alpha, \end{aligned} \quad (46)$$

$$\begin{aligned} \rho_{\parallel}^{\text{dc}-} &= \rho_f \nu_0^{\omega-} \cos^2 \alpha, \\ \rho_{\perp}^{\text{dc}-} &= \rho_f(\delta \nu_0^{\omega+} + \nu_0^{\omega-} \sin \alpha \cos \alpha). \end{aligned} \quad (47)$$

Here $\nu_0^{\omega\pm}$ are obtained from the relation

$$\nu_0^{\omega} = 1 + \langle \hat{F}_{px} \rangle_0^{\omega} / j^{\text{dc}} \equiv 1 + \text{Im } G_0, \quad (48)$$

where $G_0 \equiv \psi_0(j^{\text{dc}}, j^{\text{ac}}, \omega, g) / j^{\text{dc}}$ and

$$\nu_0^{\omega+} = 1 + \text{Im } G_0^+, \quad \nu_0^{\omega-} = \text{Im } G_0^-. \quad (49)$$

In the limit of a small Hall effect ($\epsilon \ll 1$) the expressions for even and odd components of ν_0^{ω} (in terms of G_0^{\pm}) in the linear approximation in the parameter $\epsilon \tan \alpha \ll 1$ are equal respectively to

$$\begin{aligned} G_0^+ &= G_0(n\xi_y^{\text{dc}}, n\xi_y^{\text{ac}}) + nR_d^+ \delta \tan \alpha, \\ G_0^- &= (nR_d^- - G_0^+) \delta \tan \alpha, \end{aligned} \quad (50)$$

$$R_d \equiv [\partial \psi_0 / \partial \xi_y^{\text{dc}} + (j^{\text{ac}} / j^{\text{dc}}) (\partial \psi_0 / \partial \xi_y^{\text{ac}})], \quad (51)$$

where $\psi_0 = \psi_0(n\xi_y^{\text{dc}}, n\xi_y^{\text{ac}})$, j^{dc} and j^{ac} are dc and ac density values, and R_d^+ and R_d^- are even and odd parts of the R_d , respectively.

As follows from Eqs. (46) and (47), the behavior of the dc and temperature dependence of $\rho_{\parallel, \perp}^{\text{dc}\pm}$ is completely determined by the $(j^{\text{dc}}, g | j^{\text{ac}}, \omega)$ behavior of the $\nu_0^{\omega\pm}$ dependences. If $(j^{\text{ac}} / j^{\text{dc}}) \ll 1$, i.e., the influence of the ac on the dc response is considered small, the linear limit for $E_{\parallel, \perp}^{\text{dc}\pm}(j^{\text{dc}})$ dependences, following Eqs. (46) and (47), is realized in that region of j^{dc} and g , where $\nu_0^{\omega+} = \text{const}$ and $\nu_0^{\omega-} = 0$, while the region of nonlinearity of $\rho_{\parallel, \perp}^{\text{dc}\pm}(j^{\text{dc}}, g | j^{\text{ac}}, \omega)$ dependences corresponds to those j^{dc} and g intervals, where the dependences $\nu_0^{\omega\pm}(\xi_y^{\text{dc}} | g)$ and $\nu_0^{\omega\pm}(g | \xi_y^{\text{dc}})$ are nonlinear. Note that the nonlin-

earity in the temperature dependences $\rho_{\parallel, \perp}^{\text{dc}\pm}(g | \xi_y^{\text{dc}})$ can be observed not only at small currents (in the TAFF regime) but even at large currents $\xi_y^{\text{dc}} > 1$ in the case where $\xi_y^{\text{ac}} < 1$, where this latter relation depends on the magnitude of the angle α [for $\cos \alpha < 1 / \xi_y^{\text{dc}}$ we have $\xi_y^{\text{ac}} < 1$ and $\nu_0^{\omega}(g \gg 1) = 0$]. Thus, the linearity or nonlinearity of the dependences $\rho_{\parallel, \perp}^{\text{dc}\pm}(g)$ at dcs larger than unity depends on the magnitude of the angle α .

E. Shapiro steps and adiabatic dc response

Before a discussion about the influence of the ac on the CVC of the model under discussion, it is instructive to consider first a simple physical picture of the vortex motion in a *tilted* (due to the presence of the dimensionless dc driving force $0 < \xi^{\text{dc}} < \infty$) washboard PPP under the influence of the *effective* dimensionless driving force $\hat{f} = \hat{F}_{px} + \hat{F}_{Lx} = -\sin x + \xi^{\text{dc}}$. If the temperature is zero, the vortex is at rest with $\xi^{\text{dc}} = 0$ at the bottom of the potential well of the PPP. When the PPP is gradually lowered by increasing ξ^{dc} , then for $0 < \xi^{\text{dc}} < 1$ appears an asymmetry of the left-side and right-side potential barriers for a given potential well, and in this range of ξ^{dc} an effective force \hat{f} changes its sign periodically. With gradual ξ^{dc} increase there will come a point where $\xi^{\text{dc}} = 1$; for $\xi^{\text{dc}} > 1$ the more lower right-side potential barrier disappears, the effective motive force \hat{f} becomes present everywhere along x positive and the vortex is in the “running” state, periodically changing its velocity with a dimensionless frequency $\omega_i = \sqrt{(\xi^{\text{dc}})^2 - 1}$. So the static CVC of this periodic motion at $\xi^{\text{dc}} > 1$ is a result of time averaging of the stationary time-dependent solution of the equation of motion $dx/d\tau = \hat{f}$ with $\tau = t/\hat{\tau}$. Eventually, the probability of the vortex overcoming the barriers of the PPP $\nu_0 \equiv \nu_0^{\omega}(\xi^{\text{dc}} = 0, \omega = 0)$ at zero temperature is

$$\nu_0 = \begin{cases} 0, & \xi^{\text{dc}} < 1 \\ \sqrt{1 - (1/\xi^{\text{dc}})^2}, & \xi^{\text{dc}} \geq 1, \end{cases} \quad (52)$$

i.e., the $\nu_0(\xi^{\text{dc}} > 1)$ monotonically tends to unity with increasing ξ^{dc} .

If the temperature is nonzero, a diffusionlike mode appears in the vortex motion. At low temperatures ($g \gg 1$) and $0 < \xi^{\text{dc}} < 1$ the TAFF regime of the vortex motion occurs by means of the vortex hopping between neighboring potential wells of the PPP. The intensity of these hops at low temperatures is proportional to $\exp[-g(1 - \xi^{\text{dc}})]$, i.e., strongly increases with increasing T and increasing ξ^{dc} due to the lowering of the right-side potential barriers at their tilting. On the other hand, at ξ^{dc} just above the unity (when the running mode is yet weak), the diffusionlike mode can strongly increase the average vortex velocity even at relatively low temperature due to a strong enhancement of the effective diffusion coefficient of an overdamped Brownian particle in a tilted PPP near the critical tilt¹⁸ at $\xi^{\text{dc}} = 1$ (see Sec. V H).

Now we consider the influence of a small ($\xi^{\text{ac}} \ll 1$) ac density with a frequency ω on the CVC in the limit of very small temperatures ($g \gg \gg 1$). In this case the physics of the dc response is quite different depending on the ξ^{dc} value with respect to the unity. If $\xi^{\text{dc}} < 1$, the vortex is mainly (excluding very rare hops to the neighboring wells) localized at the bot-

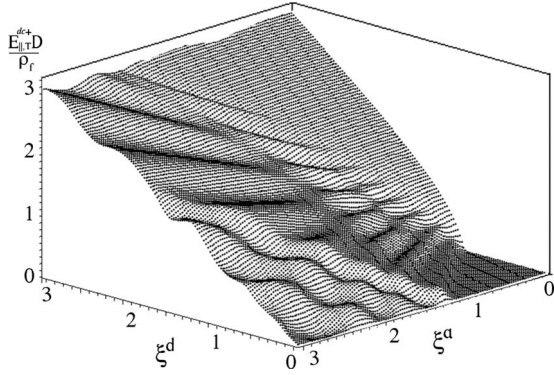


FIG. 3. The longitudinal CVC $E_{||,T}^{dc+}(\xi^d, \xi^a)$, with $\Omega=0.2, g=100$, showing the Shapiro steps.

tom of the potential well, where it experiences a small ω oscillations. The averaging of the vortex motion over the period of oscillations in this case cannot change the CVC which existed in the absence of the ac drive.

If, however, $\xi^d > 1$, then the vortex is in a running state with the internal frequency of oscillations $\omega_i = \sqrt{(\xi^d)^2 - 1}$. If $\omega \neq \omega_i$, the CVC is changed only in the second-order perturbation approach in terms of a small parameter $\xi^a \ll 1$ (as it was shown for the analogous resistively shunted Josephson-junction problem¹⁹) because the CVC is not changed in the linear approximation in this case. However, for $\omega = \omega_i$ appears a problem of a synchronization of the running vortex oscillations at the ω_i frequency with the external driving frequency ω . As a result, the average (over period of oscillations) vortex velocity is locked in with the ω in some interval of the dc density ξ^d even within the frame of the first-order perturbation calculation. The width of this first synchronization step (or the so-called Shapiro step in the resistively shunted Josephson-junction problem) was found in Ref. 20. The calculation in the spirit of this reference gives the boundaries of the ξ^d where the step occurs as

$$(\xi_\omega^d - \xi^a/2\xi^d) < \xi^d < (\xi_\omega^d + \xi^a/2\xi^d). \quad (53)$$

Here ξ_ω^d is the current density which gives $\omega_i = \sqrt{(\xi_\omega^d)^2 - 1} = \omega$, i.e., $\xi_\omega^d = \sqrt{1 + \omega^2}$. Then the size of the first Shapiro step on the CVC is ξ^a/ξ_ω^d . In higher approximations [in terms of $(\xi^a)^m$, where m runs through all of the integers] the Shapiro steps on the CVC appear at the frequencies $\Omega = m\omega$ and $\Omega_i = m\omega_i$. The width of the m th step at $\xi^a \rightarrow 0$ is proportional to $(\xi^a)^m$, i.e., strongly decreases with increasing m .²¹

In Fig. 3 we plot the longitudinal CVC $E_{||,T}^{dc+}(\xi^d, \xi^a)$ showing the Shapiro steps. The plot in Fig. 3 looks like the curves discussed earlier²² for the CVC of the microwave-driven resistively shunted Josephson-junction model at $T=0$ where the overall shape of the CVC and different behaviors of the two types of the Shapiro steps in the adiabatic limit were explained. Our graph, in comparison with the curves in Ref. 22, is smoothed due to the influence of a finite temperature. The longitudinal CVC $E_{||,T}^{dc+}(\xi^d, \xi^a)$ dependence demonstrates several main features. First, in the presence of the microwave current the dc critical current $\xi_c^d(\xi^a)$ is a decreasing function of the ac drive. The physical reason for such behavior lies in

the replacement of the dc critical current by the total dc +ac critical current. Second, with gradual ξ^a increase the zero-voltage step reduces to zero and all other steps appear. Such steps are common because they do not oscillate and spread over a dc range about twice the critical current $2\xi_c^d$. These steps are the steps of the first kind and they distort the CVC like a relief bump with a concave shift from the Ohmic line. With further ξ^a increase this relief bump shifts toward higher ξ^d values. Below this range the steps of the second kind appear. These microwave current-induced steps oscillate rapidly and stay closely along the Ohmic line²² over the dc range $\xi^d \leq \xi^a - 1$.

To summarize, we can determine three (ξ^d, ξ^a) ranges where the CVC behavior is qualitatively different. For large dc bias current densities $\xi^a + 1 < \xi^d$ the CVC asymptotically approaches the Ohmic line without microwave-induced steps. For the intermediate dc range $\xi^a - 1 < \xi^d < \xi^a + 1$ the CVC curve deviates from the Ohmic line as a concave bump with the stable steps. For the lower dc range $\xi^d < \xi^a - 1$ the steps oscillate with microwave current along the Ohmic line. With gradual Ω increase the size of the steps increases, whereas their number decreases.

V. NONLINEAR STATIONARY ac RESPONSE

A. Derivation of the impedance tensor

Using Eq. (11) we determine the nonlinear (in the amplitudes j^{ac} and j^{dc} and the frequency ω) stationary ac response as

$$\langle \mathbf{E} \rangle_t \equiv \langle \langle \mathbf{E} \rangle(t) - \langle \mathbf{E} \rangle_0^\omega \rangle = (nB/c)[\langle v_x \rangle_t \mathbf{y} - \langle v_y \rangle_t \mathbf{x}], \quad (54)$$

where $\langle \mathbf{E} \rangle_0^\omega = (nB/c)[-\langle v_y \rangle_0^\omega \mathbf{x} + \langle v_x \rangle_0^\omega \mathbf{y}]$ is time-independent part of $\langle \mathbf{E} \rangle(t)$ [see also Eqs. (26) and (29)], whereas $\langle v_y \rangle_t$ and $\langle v_x \rangle_t$ are time-dependent periodic parts of $\langle v_y \rangle(t)$ and $\langle v_x \rangle(t)$ which become zero after averaging over a period of $2\pi/\omega$ of the ac cycle.

From Eqs. (13) and (54) we have

$$\langle E_y \rangle_t = (n\rho_f j_c / D) \sum_{k=1}^{\infty} (j^{ac})^k \text{Re}\{Z_k(\omega) e^{ik\omega t}\}, \quad (55)$$

where

$$Z_k(\omega) = \delta_{1,k} - i\psi_k(\omega)/(j^{ac})^k, \quad (56)$$

$$\psi_k(\omega) \equiv [F_k^1(\omega) - F_k^{-1}(\omega)],$$

and $\delta_{1,k}$ is Kronecker's delta.

The dimensionless transformation coefficients Z_k in Eq. (55) have a physical meaning as the k th harmonic with frequency $\Omega_k \equiv k\omega$ in the ac nonlinear $\langle E_y \rangle_t$ response. Equation (56) for $k=1$ yields

$$Z_1 = 1 - i\psi_1/j^{ac}. \quad (57)$$

Using Eqs. (54) and (55) we can express the nonlinear stationary ac response on the ω -frequency E_{y1}^{ac} in terms of the nonlinear impedance Z_1 as

$$E_{y1}^{\text{ac}} = (\rho_f/D)(j_y^{\text{ac}} + \delta j_x^{\text{ac}})\text{Re}\{Z_1 e^{i\omega t}\}. \quad (58)$$

If we put $Z_1 \equiv \rho_1 - i\zeta_1$, where ρ_1 and ζ_1 are the dynamic resistivity and the reactivity, respectively, then Eq. (58) acquires the form

$$E_{y1}^{\text{ac}} = (\rho_f/D)(j_y^{\text{ac}} + \delta j_x^{\text{ac}})\sqrt{\rho_1^2 + \zeta_1^2} \cos(\omega t - \varphi_1), \quad (59)$$

where $\sqrt{\rho_1^2 + \zeta_1^2} \equiv |Z_1|$ and $\varphi_1 = \arctan(\zeta_1/\rho_1)$ are the dimensionless amplitude and phase of the ac response on the $j_{Lx}^{\text{ac}} = (j_y^{\text{ac}} + \delta j_x^{\text{ac}})\cos \omega t$ input.

Similarly, using Eqs. (12) and (54), we can show that

$$\langle E_x \rangle_t = \rho_f j_x^{\text{ac}} \cos \omega t - \delta \langle E_y \rangle_t, \quad (60)$$

and obtain the ω -frequency ac response E_{x1}^{ac} as

$$E_{x1}^{\text{ac}} = (\rho_f/D)\text{Re}\{e^{i\omega t}[(D - \delta^2 Z_1)j_x - \delta Z_1 j_y]\}. \quad (61)$$

From Eqs. (58) and (61) it follows that the complex amplitudes of the electric field \mathbf{E}_1 and the current density $\mathbf{J} = \mathbf{j}e^{i\omega t}$ are connected by the relation $\mathbf{E}_1 = \hat{Z}\mathbf{J}$, where \hat{Z} is the frequency- and dc and ac amplitude-dependent impedance tensor,

$$\hat{Z}(\omega) = \begin{pmatrix} Z_{xx} & Z_{xy} \\ Z_{yx} & Z_{yy} \end{pmatrix} = \frac{\rho_f}{D} \begin{pmatrix} D - \delta^2 Z_1 & -\delta Z_1 \\ \delta Z_1 & Z_1 \end{pmatrix}. \quad (62)$$

It is relevant to note the similarity between Eqs. (30) and (62), from which follows that for the ac response Z_1 plays the same role as ν_0^ω for the dc response.

However, the connection between Z_1 and the dynamical average pinning force $\langle \hat{F}_{px} \rangle_{t1}$ is more complex than the relation between ν_0^ω and $\langle \hat{F}_{px} \rangle_0^\omega$ [see Eq. (28)]. Taking into account the time dependence of the $\langle \hat{F}_{px} \rangle_{t1}$, it is easy to show that

$$\langle \hat{F}_{px} \rangle_{t1} = \text{Re}\{e^{i\omega t}[j^{\text{ac}}(Z_1 - 1)]\}. \quad (63)$$

Equation (63) gives a physical interpretation of the Z_1 impedance and its structure may be compared with Eq. (28).

The real quantities $\mathbf{E}_1 = \text{Re} \mathbf{E}_1$ and $\mathbf{j}^{\text{ac}} = \text{Re} \mathbf{J}$ are connected by the relation $\mathbf{E}_1 = \hat{\rho}^{\text{ac}} \mathbf{j}$, where the ac-response resistivity tensor is

$$\hat{\rho}^{\text{ac}} = \begin{pmatrix} \rho_{xx}^{\text{ac}} & \rho_{xy}^{\text{ac}} \\ \rho_{yx}^{\text{ac}} & \rho_{yy}^{\text{ac}} \end{pmatrix}. \quad (64)$$

Note that from Eqs. (58) and (61) it follows that

$$\hat{\rho}^{\text{ac}} = \text{Re}\{\hat{Z}(\omega)e^{i\omega t}\}. \quad (65)$$

B. Longitudinal and transverse impedance responses

The experimentally measurable ac resistive responses refer to the coordinate system to which the ac is directed, for simplicity, at the same angle α with respect to the y axis as the dc (see Fig. 1). The longitudinal and transverse (with respect to the ac direction) components of the electric field, $E_{\parallel}^{\text{ac}}$ and E_{\perp}^{ac} , are related to $E_x^{\text{ac}}(t)$ and $E_y^{\text{ac}}(t)$ by the same

relations as for the dc [see Eq. (37)]. The latter is true for the relations between the experimentally observable longitudinal and transverse (with respect to the \mathbf{j}^{ac} direction) magnetoresistivities $\rho_{\parallel}^{\text{ac}} = E_{\parallel}^{\text{ac}}/j^a$ and $\rho_{\perp}^{\text{ac}} = E_{\perp}^{\text{ac}}/j^a$, where j^a is j^{ac} amplitude [$(j^a)^2 = (j_x^{\text{ac}})^2 + (j_y^{\text{ac}})^2$]. As a result we have

$$\rho_{\parallel}^{\text{ac}} = \text{Re}\{Z_{\parallel} e^{i\omega t}\}, \quad \rho_{\perp}^{\text{ac}} = \text{Re}\{Z_{\perp} e^{i\omega t}\}, \quad (66)$$

where

$$Z_{\parallel} = (\rho_f/D)[(D - \delta^2 Z_1)\sin^2 \alpha + Z_1 \cos^2 \alpha],$$

$$Z_{\perp} = (\rho_f/D)[\delta Z_1 - D(1 - Z_1)\cos \alpha \sin \alpha]. \quad (67)$$

Note, however, that the magnitudes of the $\rho_{\parallel}^{\text{ac}}$ and ρ_{\perp}^{ac} , given by Eq. (66), in general (as in the case of dc) depend on the direction of the external magnetic field \mathbf{B} along the z axis due to the $\delta = n\epsilon$ dependence of the Z_1 through the implicit dependence of $\psi_1(\omega)$ on the j^{ac} and j^{dc} . In order to consider only n -independent magnitudes of the $\rho_{\parallel}^{\text{ac}}$ and ρ_{\perp}^{ac} resistivities, we should introduce the even (+) and odd (−) longitudinal and transverse magnetoresistivities with respect to magnetic-field reversal in the form $\rho_{\parallel,\perp}^{\text{ac}\pm}(n) \equiv [\rho_{\parallel,\perp}^{\text{ac}}(n) \pm \rho_{\parallel,\perp}^{\text{ac}}(-n)]/2$.

Let us first separate $Z_1 = 1 - i\psi_1/j^{\text{ac}}$ into the even $Z_1^+(n) = Z_1^+(-n)$ and the odd $Z_1^-(n) = -Z_1^-(-n)$ parts. If we assume $\psi_1(n) = \psi_1^+(n) + \psi_1^-(n)$, where $\psi_1^{\pm}(n)$ are the even and odd parts of $\psi_1(n)$ (i.e., $\psi_1^{\pm}(n) = [\psi_1(n) \pm \psi_1(-n)]/2$), then we have

$$Z_1^+(n) = 1 - inj_c[j_y \psi_1^-(n) - \delta j_x \psi_1^+(n)]/(j_y^2 - \delta^2 j_x^2),$$

$$Z_1^-(n) = -inj_c[j_y \psi_1^+(n) - \delta j_x \psi_1^-(n)]/(j_y^2 - \delta^2 j_x^2). \quad (68)$$

From now on, we can present Eq. (67) in a form similar to Eqs. (39) and (40) with the only difference as the change of ν_0^{\pm} to Z_1^{\pm} and $\rho_{\parallel,\perp}^{\text{dc}\pm}$ to $Z_{\parallel,\perp}^{\pm}$. However, hereafter it will be suitable for us to present Eq. (67) in another equivalent form,

$$Z_{\parallel}^+ = (\rho_f/D)[(D - \delta^2 Z_1^+)\sin^2 \alpha + Z_1^+ \cos^2 \alpha], \quad (69)$$

$$Z_{\parallel}^- = (\rho_f/D)Z_1^-(\cos^2 \alpha - \delta^2 \sin^2 \alpha), \quad (70)$$

$$Z_{\perp}^+ = (\rho_f/D)[\delta Z_1^- - D(1 - Z_1^+)\sin \alpha \cos \alpha], \quad (71)$$

$$Z_{\perp}^- = (\rho_f/D)(\delta Z_1^+ + DZ_1^- \sin \alpha \cos \alpha). \quad (72)$$

C. Hall effect and the guiding of vortices in nonlinear ac response

Let us consider peculiarities of the ac resistive responses in the investigated model due to the Hall effect. Experimentally, three types of measurements of the observed ac resistive characteristics are possible in a prescribed geometry defined by a fixed value of the angle α . First is ac-response measurements which investigate the dependence of observed $\rho_{\parallel,\perp}^{\text{ac}\pm}(\xi^a | \xi^d, g)$ resistivities on the current density ξ^a at fixed dc density ξ^d and inverse temperature g . Second is the dependence of $\rho_{\parallel,\perp}^{\text{ac}\pm}(g | \xi^a, \xi^d)$ on the inverse temperature at fixed ξ^a and ξ^d . Third, is the dependence of $\rho_{\parallel,\perp}^{\text{ac}\pm}(\xi^d | \xi^a, g)$ on

the dc density at fixed ξ^a and g . The form of these dependences is governed by a geometrical factor—the angle α between the directions of the current-density vector $\mathbf{j}(t)$ and the channels of the washboard pinning potential. There are two different forms of the dependence of $\rho_{\parallel,\perp}^{\text{ac}\pm}$ on the angle α [see formulas (69)–(72)]. The first of these is the “tensor” dependence, also present in the linear regimes [similar to the TAFF and FF regimes for formulas (39) and (40)], which is external to the impedance Z_1 [see Eq. (67)]. The second is through the dependence of Z_1 on its arguments $\xi^a(\alpha)$ and $\xi^d(\alpha)$, which in the region of the transition from linear in j^{ac} and j^{dc} regimes (at $\xi^{a,d} \ll 1$ and $\xi^{a,d} \gg 1$) is substantially nonlinear.

First recall that in the absence of the Hall effect ($\epsilon=0$) there exist only even (with respect to magnetic-field inversion) impedances $Z_{\parallel,\perp}^+$ —the odd impedances $Z_{\parallel,\perp}^-$ are zero [see Eqs. (69)–(72)]. The presence of nonzero value of ϵ leads not only to the appearance of a Hall contribution to the observed ac responses on account of the even component Z_1^+ of the impedance Z_1 , but also to the appearance of the odd component Z_1^- , which has a maximum in the region of the nonlinear transition from one linear regime (at low ξ^a, ξ^d and $g \gg 1$) to another linear regime (at large ξ^a, ξ^d and arbitrary g) and is essentially equal to zero outside this transitional region (see Figs. 10 and 11 of Ref. 3). As a consequence, “crossover” effects arise: contributions from Z_1^- to effects due to Z_1^+ and vice versa, and contributions from Z_1^+ to effects due to Z_1^- . Thus, in the even impedance $Z_{\parallel,\perp}^+$ [see Eq. (71)], in addition to the main contribution created by the guiding of vortices and described by Z_1^+ , there exists a Hall contribution arising due to Z_1^- . The expression for the odd impedance $Z_{\parallel,\perp}^-$ [see Eq. (72)] contains, in addition to the Hall term arising due to Z_1^+ , a term due to Z_1^- .

D. ac response in LT geometries

In order to study a simpler form of Eqs. (69)–(72) we consider first the L and T geometries of the ac response (see Fig. 1, inset). In L geometry $\alpha = \pi/2$ and $j_L^{\text{ac}} = \epsilon \xi^a$ does not depend on n as well as $j_L^{\text{dc}} = \epsilon \xi^d$ for the dc. As a result, $\psi_{1,L}$ as well as $Z_{1,L} = 1 - i\psi_{1,L}/j_L^{\text{ac}}$ have $\psi_{1,L}^- = Z_{1,L}^- = 0$. Finally, from Eq. (69) it follows that

$$Z_{\parallel,L}^+ = (\rho_f/D)[1 + \delta^2(1 - Z_{1,L}^+)], \quad Z_{\parallel,L}^- = 0, \quad (73)$$

$$Z_{\perp,L}^+ = 0, \quad Z_{\perp,L}^- = \delta(\rho_f/D)Z_{1,L}^+. \quad (74)$$

If we define $\rho_{\parallel,L}^{\text{ac}+}$ and $\zeta_{\parallel,L}^{\text{ac}+}$ as the resistivity and reactivity of $Z_{\parallel,L}^+$ impedance, respectively, by using the relation $Z_{\parallel,L}^+ = \rho_{\parallel,L}^{\text{ac}+} - i\zeta_{\parallel,L}^{\text{ac}+}$ we can show that

$$\begin{aligned} \rho_{\parallel,L}^{\text{ac}+} &= (\rho_f/D)(1 - \epsilon \text{Im} \psi_{1,L}/\xi^a), \\ \zeta_{\parallel,L}^{\text{ac}+} &= -(\rho_f/D)\epsilon \text{Re} \psi_{1,L}/\xi^a. \end{aligned} \quad (75)$$

Note that experimentally measured quantities of $|Z_{\parallel,L}^+|$ and $\tan \varphi_{\parallel,L} = \zeta_{\parallel,L}^{\text{ac}+}/\rho_{\parallel,L}^{\text{ac}+}$ allow one to obtain $\rho_{\parallel,L}^{\text{ac}+}$ and $\zeta_{\parallel,L}^{\text{ac}+}$ and to compare them with the theoretical formulas in Eq. (75). Similar calculations for $Z_{\perp,L}^- = \rho_{\perp,L}^{\text{ac}-} - i\zeta_{\perp,L}^{\text{ac}-}$ yield

$$\rho_{\perp,L}^{\text{ac}-} = n(\rho_f/D)(\epsilon \xi^a - \text{Im} \psi_{1,L})/\xi^a,$$

$$\zeta_{\perp,L}^{\text{ac}-} = n(\rho_f/D)\text{Re} \psi_{1,L}/\xi^a. \quad (76)$$

In T geometry (see inset of Fig. 1) $\alpha=0$, $j_T^{\text{ac}} = n\xi^a$, and $j_T^{\text{dc}} = n\xi^d$. In this case it follows from Eqs. (20)–(23) that $\psi_{1,T}(n) = -\psi_{1,T}(-n)$, i.e., $\psi_{1,T}$ is an odd function of n and $\psi_{1,T}^+ = 0$. As a result,

$$Z_{1,T}^+ = 1 - in\psi_{1,T}^-/\xi^a, \quad Z_{1,T}^- = 0. \quad (77)$$

Then from Eqs. (69)–(72) we have

$$Z_{\parallel,T}^+ = (\rho_f/D)Z_{1,T}^+, \quad Z_{\parallel,T}^- = 0, \quad (78)$$

$$Z_{\perp,T}^- = (\rho_f/D)\delta Z_{1,T}^+, \quad Z_{\perp,T}^+ = 0. \quad (79)$$

If $Z_{\parallel,T}^+ = \rho_{\parallel,T}^{\text{ac}+} - i\zeta_{\parallel,T}^{\text{ac}+}$ and $Z_{\perp,T}^- = \rho_{\perp,T}^{\text{ac}-} - i\zeta_{\perp,T}^{\text{ac}-}$, then from Eqs. (78) and (79) we obtain $Z_{\perp,T}^- = \delta Z_{\parallel,T}^+$ and

$$\rho_{\perp,T}^{\text{ac}-} = \delta\rho_{\parallel,T}^{\text{ac}+}, \quad \zeta_{\perp,T}^{\text{ac}-} = \delta\zeta_{\parallel,T}^{\text{ac}+}. \quad (80)$$

From Eq. (80) it follows that experimentally measured quantities satisfy the simple relations

$$|Z_{\perp,T}^-| = \epsilon|Z_{\parallel,T}^+|, \quad \tan \varphi_{\perp,T}^- = \tan \varphi_{\parallel,T}^+. \quad (81)$$

At last, from Eqs. (77) and (78) it follows that $\rho_{\parallel,T}^{\text{ac}+} = (\rho_f/D)\rho_{1,T}^{\text{ac}+}$ and $\zeta_{\parallel,T}^{\text{ac}+} = (\rho_f/D)\zeta_{1,T}^{\text{ac}+}$, where

$$\rho_{1,T}^{\text{ac}+} = 1 + n \text{Im} \psi_{1,T}^-/\xi^a,$$

$$\zeta_{1,T}^{\text{ac}+} = n \text{Re} \psi_{1,T}^-/\xi^a, \quad \rho_{1,T}^- = \zeta_{1,T}^- = 0. \quad (82)$$

E. Power absorption in ac response

In order to calculate the power absorbed per unit volume \bar{P} (and averaged over the period of an ac cycle), we use the standard relation $\bar{P} = (1/2)\text{Re}(\mathbf{E}_1 \cdot \mathbf{J})$, where \mathbf{E}_1 and \mathbf{J} are the complex amplitudes of the ac electric field and current density, respectively. Using Eqs. (62) and (67) we can show that

$$\bar{P} = (j^2/2)\bar{\rho} \equiv (j^2/2)\text{Re} Z_{\parallel}. \quad (83)$$

After some algebra we obtain

$$\bar{\rho} = (\rho_f/D)[D \sin^2 \alpha + (1 - D \sin^2 \alpha)\text{Re} Z_1]. \quad (84)$$

Taking into account that $Z_1 \equiv 1 - iG_1$, where $G_1 \equiv \psi_1/j^{\text{ac}}$, we conclude that $\text{Re} Z_1 = 1 - \text{Re}(iG_1) = 1 + \text{Im} G_1$. Then from Eq. (84) we have

$$\bar{\rho} = (\rho_f/D)[1 + (1 - D \sin^2 \alpha)\text{Im} G_1]. \quad (85)$$

In the limit of $\epsilon \ll 1$ we obtain for $\bar{\rho}$ a simpler result,

$$\bar{\rho} = \rho_f(1 + \text{Im} G_1 \cos^2 \alpha), \quad (86)$$

which will be analyzed in detail in Sec. IV F.

From Eq. (84) follows two simple results for $\bar{\rho}$ in LT geometries,

$$\bar{\rho}_L = (\rho_f/D)(D - \delta^2 \text{Re } Z_{1L}) = (\rho_f/D)(1 - \epsilon \text{Im } \psi_{1L}/\xi^a), \quad (87)$$

$$\bar{\rho}_T = (\rho_f/D)\text{Re } Z_{1T} = (\rho_f/D)(1 + n \text{Im } \psi_{1T}^-/n\xi^a). \quad (88)$$

Note that $\bar{\rho}_L$ and $\bar{\rho}_T$ in Eqs. (87) and (88) are equal to the expressions for the $\rho_{\parallel,L}^{\text{ac}}$ and $\rho_{\parallel,T}^{\text{ac}}$ given by Eqs. (75) and (82), respectively.

F. ac impedance and power absorption at $\epsilon \ll 1$

Here we analyze the ac+dc impedance dependences Z_{\parallel}^{\pm} and Z_{\perp}^{\pm} [see Eqs. (69)–(72)], with allowance for the small Hall effect ($\epsilon \ll 1$). In this case Eqs. (69)–(72) become simpler and the expressions for $Z_{\parallel,\perp}^{\pm}$, out of terms of order $\epsilon^2 \ll 1$, have the form

$$Z_{\parallel}^+ = \rho_f(Z_1^+ \cos^2 \alpha + \sin^2 \alpha),$$

$$Z_{\perp}^+ = \rho_f(Z_1^+ - 1) \sin \alpha \cos \alpha, \quad (89)$$

$$Z_{\parallel}^- = \rho_f Z_1^- \cos^2 \alpha,$$

$$Z_{\perp}^- = \rho_f(\delta Z_1^+ + Z_1^- \sin \alpha \cos \alpha). \quad (90)$$

Here Z_1^{\pm} can be obtained from relation

$$Z_1 = Z_1^+ + Z_1^- = 1 - iG_1 = 1 - i(G_1^+ + G_1^-) = (1 - iG_1^+) - iG_1^-, \quad (91)$$

where $G_1 \equiv \psi_1(j^{\text{ac}}, j^{\text{dc}})/j^{\text{ac}}$, $Z_1^+ = (1 - iG_1^+)$, and $Z_1^- = -iG_1^-$. In the case of a small Hall effect ($\epsilon \ll 1$) the expressions for even (+) and odd (−) components of $Z_1(\xi^{\text{ac}}, \xi^{\text{dc}})$ (in terms of G_1^{\pm}) in the linear approximation in the parameter $\epsilon \tan \alpha \ll 1$ are equal respectively to

$$G_1^+ = G_1(n\xi_y^a, n\xi_y^d) + nR_a^+ \delta \tan \alpha,$$

$$G_1^- = (-G_1^+ + nR_a^-) \delta \tan \alpha, \quad (92)$$

$$R_a \equiv [(\partial\psi_1/\partial\xi_y^a) + (j^d/j^a)(\partial\psi_1/\partial\xi_y^d)], \quad (93)$$

where $\psi_1 = \psi_1(n\xi_y^a, n\xi_y^d)$, j^a and j^d are ac and dc density values, and R_a^+ and R_a^- are even and odd parts of the R_a , respectively.

It is worth noticing that Eqs. (89) and (90) have the same structure as Eqs. (46) and (47) for the dc+ac response at ϵ

$\ll 1$. Actually, if we change Z_1^{\pm} and $Z_{\parallel,\perp}^{\pm}$ in Eqs. (89) and (90) to $\nu_0^{\omega\pm}$ and $\rho_{\parallel,\perp}^{\text{dc}\pm}$, respectively, we obtain then Eqs. (46) and (47). So all conclusions following the discussion about the structure of these equations can be repeated for Eqs. (89) and (90).

It is interesting also to analyze an anisotropic power absorption in the limit of $\epsilon \ll 1$, given by Eq. (86) in Sec. IV E. Let us set $G_1 = G_1^+ + G_1^-$, where G_1^{\pm} are presented by Eqs. (92) and (93). In the case where $\epsilon = 0$, $G_1 = G_1^+ = G_1(n\xi_y^a, n\xi_y^d) = \psi_1(n\xi_y^a, n\xi_y^d)/n\xi_y^a$, where $\xi_y^a = \xi^a \cos \alpha$, $\xi_y^d = \xi^d \cos \alpha$, and

$$\bar{\rho} = \rho_f[1 + \cos \alpha \cdot n \text{Im } \psi_1^-/n\xi^a]. \quad (94)$$

Note that Eq. (94) at $\alpha = 0$ yields $\bar{\rho} = \bar{\rho}_T(\epsilon = 0)$, where $\bar{\rho}_T$ is given by Eq. (88).

G. Linear ac response

Here we assume that $j = j^{\text{dc}} + j^{\text{ac}} e^{i\omega t}$ and the alternating current is small ($j^{\text{ac}} \ll 1$). There are *three* different ways to derive *linear* (in j^{ac}) impedance Z_{1l} at arbitrary value of j^{dc} .

The first way is to use the general expression for $Z_1(j^{\text{ac}}, j^{\text{dc}})$ [see Eq. (57)] derived through the method of *matrix* continued fraction at arbitrary magnitudes of the j^{ac} and j^{dc} . If we take into account that $\psi_1(j^{\text{ac}} = 0) = 0$, then it follows that

$$Z_{1L} = \lim_{j^{\text{ac}} \rightarrow 0} Z_1 = 1 - i(d\psi_1/dj^{\text{ac}})|_{j^{\text{ac}}=0}. \quad (95)$$

This method is the most general and powerful if we can calculate $Z_1(j^{\text{ac}}, j^{\text{dc}})$.

The second way is to calculate Z_{1l} by means of making the perturbation expansion of the $\langle r^m \rangle(t)$ [see Eq. (10)] in powers of $j^{\text{ac}} \ll 1$ in the form

$$\langle r^m \rangle_t = \langle r^m \rangle_0 + \langle r^m \rangle_1 + \dots, \quad (96)$$

where $\langle r^m \rangle_1 = A_m(\omega) j^{\text{ac}} e^{i\omega t}$, the subscript “0” denotes the statistical averages in the absence of the ac, and the subscript “1” denotes the portion of the statistical average which is linear in the ac. Whereas the $\langle r^m \rangle_0$ satisfies Eq. (32), the complex amplitude $A_m(\omega)$ (for $m \geq 1$) can be presented (see details in Sec. 5.5 of Ref. 14) in terms of the infinite scalar continued fraction $\tilde{S}_m(\omega)$ as

$$A_1(\omega) = 2i \sum_{n=1}^{\infty} (-1)^n \prod_{m=1}^n S_m \tilde{S}_m(\omega), \quad (97)$$

where

$$\tilde{S}_m(\omega) = \frac{1/2}{\frac{i\omega\hat{\tau}}{m} + ij^{\text{dc}} + \frac{m}{g} + \frac{1/4}{\frac{i\omega\hat{\tau}}{m+1} + ij^{\text{dc}} + \frac{m+1}{g} + \frac{1/4}{\frac{i\omega\hat{\tau}}{m+2} + ij^{\text{dc}} + \frac{m+2}{g} + \dots}}} \quad (98)$$

and $\tilde{S}_m(\omega=0)=S_m$ [see also Eqs. (33) and (34)]. Using Eq. (97) and taking into account that $A_{-1}(\omega)=-A_1^*(-\omega)$, we conclude that

$$\langle \sin x \rangle_1 = (i/2)(\langle r \rangle_1 - \langle r^{-1} \rangle_1) = B(\omega)j^{\text{ac}}e^{i\omega t}, \quad (99)$$

where $B(\omega) \equiv (i/2)[A_1(\omega) + A_1^*(-\omega)]$. Then from expressions for the $\langle v_x \rangle_{1l}$, taken at $j^{\text{ac}}e^{i\omega t}$ [Eqs. (63) and (99)], it follows that dimensionless linear impedance is

$$Z_{1l}(\omega) = 1 - B(\omega). \quad (100)$$

At last, the third way to calculate the linear impedance gives an approximate *analytical* expression for $Z_{1l}(\omega)$ within the frames of the method of effective eigenvalue (see details in Secs. 5.6 and 5.7 of Ref. 14). Following this approach we can express the dimensionless linear impedance in terms of the modified Bessel functions $I_\nu(z)$ as

$$Z_{1l}(\omega, g, j^{\text{dc}}) = 1 - \frac{1}{2} \left[\frac{I_{1+\mu}(g)}{I_\mu(g)(\lambda + i\omega\hat{\tau})} + \frac{I_{1-\mu}(g)}{I_{-\mu}(g)(\lambda^* + i\omega\hat{\tau})} \right], \quad (101)$$

where

$$\lambda = I_\mu(g)I_{1+\mu}(g) / \left[2 \int_0^g I_\mu(t)I_{1+\mu}(t)dt \right] \quad (102)$$

is an effective eigenvalue¹⁴ and $\mu \equiv igj^{\text{dc}}$. It follows from Eqs. (101) and (102) that at $\omega=0$

$$Z_{1l}(\omega=0, g, j^{\text{dc}}) = d[j^{\text{dc}}\nu_0(j^{\text{dc}})]/dj^{\text{dc}} = 1 - \text{Re} \left\{ [2/I_\mu^2(g)] \int_0^g I_\mu(t)I_{1+\mu}(t)dt \right\}, \quad (103)$$

where $\nu_0(j^{\text{dc}})$ is given by Eq. (35). Note also that the right-hand side of Eq. (103) is the exact expression for the dimensionless static differential resistivity in an analytical form. In the limit $j^{\text{dc}}=0$ from Eq. (103) follows the well-known result of Coffey and Clem¹¹ (see also Refs. 12 and 13). Actually, in this limit $\mu=0$ and

$$\lambda = \lambda^* = I_0(g)I_1(g)/[I_0^2(g) - 1]. \quad (104)$$

As a result

$$Z_{1l}(\omega, g, j^{\text{dc}}=0) \equiv Z_{1l}^0 = \frac{\nu_{00} + (\omega\tau)^2 + i\omega\tau(1 - \nu_{00})}{1 + (\omega\tau)^2}, \quad (105)$$

where $\nu_{00} \equiv \nu_0(j^{\text{dc}}=0) = 1/I_0^2(g)$ is the flux creep factor^{3,4,11,12} and

$$\tau = \hat{\tau}/\lambda = \hat{\tau}[I_0^2(g) - 1]/I_0(g)I_1(g) = \hat{\tau}(1 - \nu_{00})[I_0(g)/I_1(g)] \quad (106)$$

is the characteristic relaxation time. If $Z_{1l}^0 = \rho_{1l}^0 - i\xi_{1l}^0$, where ρ_{1l}^0 and ξ_{1l}^0 are linear resistivity and reactivity in the absence of the dc, respectively, then from Eq. (105) [see also Eq. (2)] it follows that

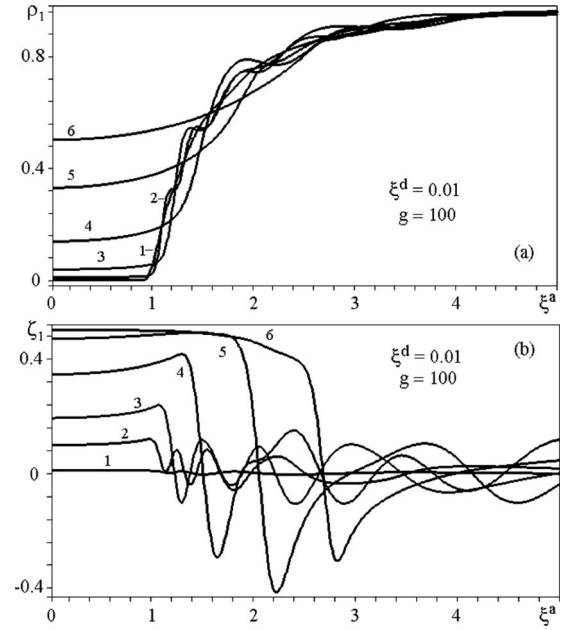


FIG. 4. The ac resistivity ρ_1 and reactivity ζ_1 versus ξ^a for $\Omega = 0.01(1), 0.1(2), 0.2(3), 0.4(4), 0.7(5), 1(6)$, with $\xi^d=0.01, g=100$.

$$\rho_{1l}^0(\omega, g) = 1 - \frac{1 - \nu_{00}}{1 + (\omega\tau)^2}, \quad \xi_{1l}^0 = -\frac{\omega\tau(1 - \nu_{00})}{1 + (\omega\tau)^2}. \quad (107)$$

As expected, in the limit of zero temperature ($g \rightarrow \infty$) we have $\nu_{00} \rightarrow 0, \tau \rightarrow \hat{\tau}$ and the results of Gittleman and Rosenblum¹⁰ [see also Eqs. (1) and (2)] follow from Eq. (107).

H. Nonlinear impedance and harmonic response

Let us consider strong nonlinear effects in the ac impedance of a sample subjected to a pure ac drive dimensionless current density $\xi^a \cos \omega t$, where $\xi^a \equiv |\mathbf{j}^{\text{ac}}|/j_c$. In the following we will discuss the behavior of $(\xi^d, \xi^a, \Omega, g)$ -dependent impedance for simplicity in terms of the dimensionless ac resistivity $\rho_1^{\text{ac}+} = \rho_1$ and reactivity $\zeta_1^{\text{ac}+} = \zeta_1$. As the angular α anisotropy in these responses is omitted, the experimental observation of the following dependences (see Figs. 4–8) can be carried out in fact by the measurement of the $\rho_{\parallel, T}^{\text{ac}+}$ and $\zeta_{\parallel, T}^{\text{ac}+}$ responses in T geometry [see Eqs. (77) and (78) and the definition of the $Z_{\parallel, T}^+$]. Figure 4 shows the dimensionless ac resistivity ρ_1 and reactivity ζ_1 versus ac density ξ^a for different dimensionless frequencies $\Omega \equiv \omega\hat{\tau}$ at very low temperature ($g=100$).

As can be seen from Fig. 4(a), when Ω is very small, the $\rho_1(\xi^a)$ shows several characteristic features: a threshold ξ_c^a value and a subsequent parabolic rise, above the threshold, with associated steplike structures. The threshold current density at which a sudden increase in $\rho_1(\xi^a)$ starts may be defined as critical current density ξ_c^a . The step height decreases with increasing ξ^a . The reactivity $\zeta_1(\xi^a)$ shows nearly periodic dynamic 2π jumps of the vortex coordinate occurring as the drive current density ξ^a is increased [see Fig. 4(b)]. The curves in Figs. 4(a) and 4(b) look like the curves discussed earlier²³ for the nonlinear resistance and reactance

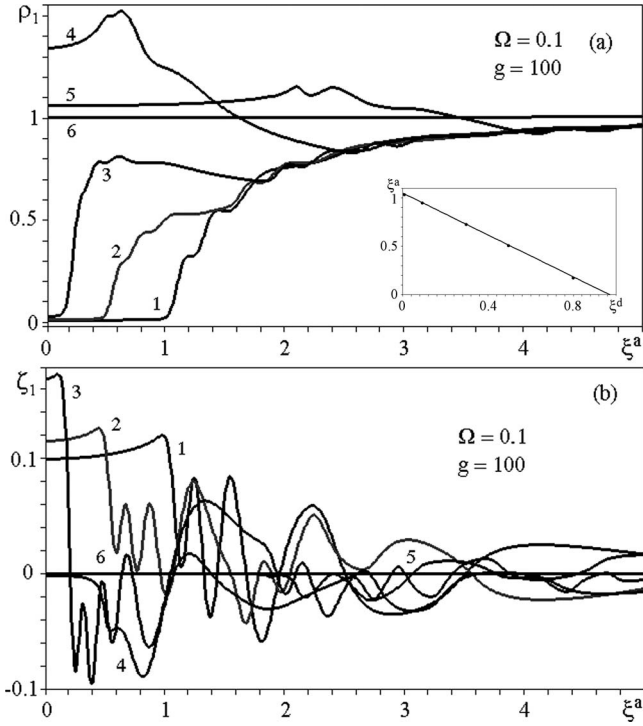


FIG. 5. The ac resistivity ρ_1 and reactivity ζ_1 versus ξ^a for $\xi^d = 0.01(1), 0.5(2), 0.8(3), 1.5(4), 3(5), 10(6)$, with $g = 100, \Omega = 0.1$.

of the purely ac-driven resistively shunted Josephson-junction model at $T=0$, where the overall shape and phase slips of these curves at several dimensionless frequencies were explained in terms of the bifurcations in the time-dependent solution of the equation for the phase difference φ across the junction.^{24,25} Analogous bifurcations of the dimensionless coordinate x versus dimensionless time $\hat{\tau}/\pi$ in our problem at $T=0$ can be calculated too.

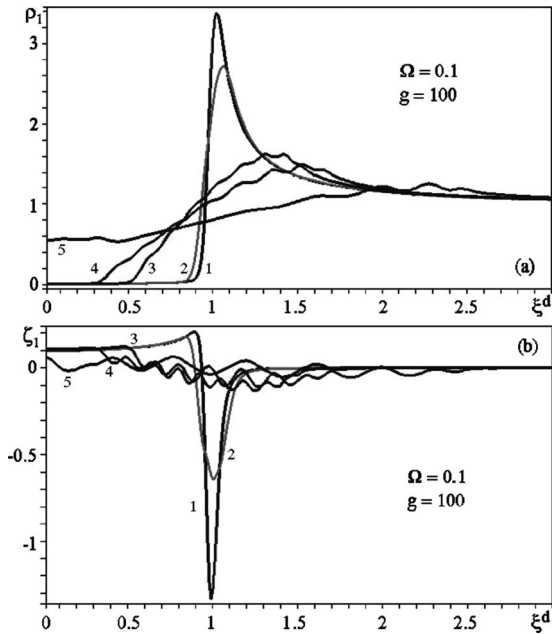


FIG. 6. The ac resistivity ρ_1 and reactivity ζ_1 versus ξ^d for $\xi^a = 0.01(1), 0.1(2), 0.5(3), 0.7(4), 1.5(5), 10(6)$, with $g = 100, \Omega = 0.1$.

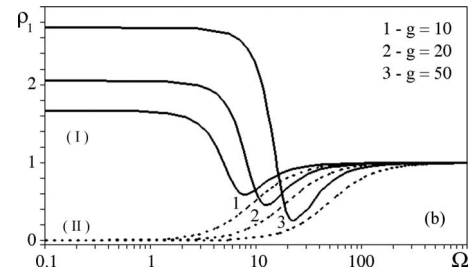


FIG. 7. The frequency dependence of $\rho_{1,T}^+(\Omega)$ for various g , (I) $\xi^d = 1$ (solid lines), (II) $\xi^d = 0$ (dotted lines).

These bifurcations can cause sudden changes in $E_{y1}^{ac}(t)$ during one cycle of the alternating current and hence result in steps.²³ When Ω becomes large, both the threshold and steps in $\rho_1(\xi^a)$ disappear and the amplitude of the x jump in $\zeta_1(\xi^a)$ becomes larger. Also, the x jump moves to large values of ξ^a and the spacing in ξ^a between bifurcations becomes large, which results in ρ_1 and ζ_1 approaching unity. Because in our problem the abrupt 2π jumps of the dimensionless vortex coordinate x correspond to the overcoming by vortex of the potential barrier between two neighboring potential wells at nonzero temperature, our curves $\rho_1(\xi^a)$ and $\zeta_1(\xi^a)$ in comparison with the curves in Refs. 24 and 25 are smoothed due to the influence of a finite temperature.

It is worth noticing that the magnitude of $\rho_1(\xi^a|\Omega)$ in Fig. 4(a) at $\xi^a < 1$ is approximately equal to a constant which progressively increases with increasing Ω . From a physical viewpoint it corresponds to the enhancement of power absorption with the growth of Ω due to the increase in the viscous losses accordingly to GR (see Sec. I) mechanism.

Now we consider the case where an ac-driven sample is dc biased, i.e., the washboard pinning potential is tilted. In Fig. 5 we plot ρ_1 and ζ_1 versus ξ^a for various values of

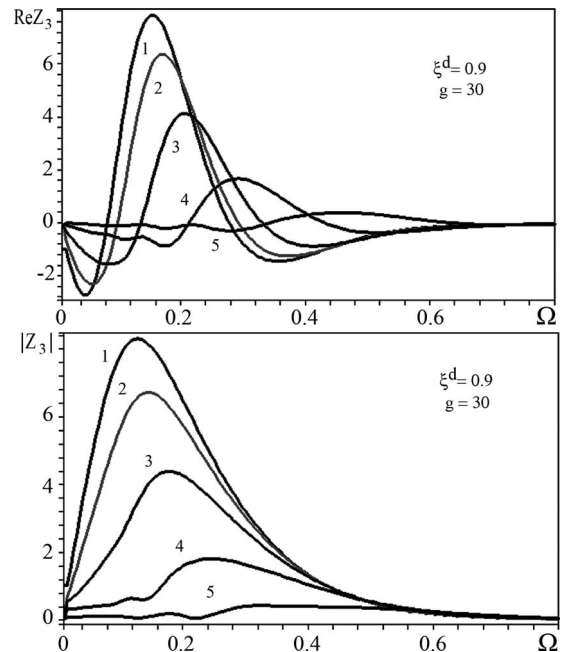


FIG. 8. The third-harmonic response $\text{Re } Z_3$ and $|Z_3|$ versus Ω for $\xi^a = 0.01(1), 0.1(2), 0.3(3), 0.5(4), 0.7(5)$, with $\xi^d = 0.9, g = 30$.

$\xi^d \equiv |j^{dc}|/j_c$ at fixed dimensionless frequency $\Omega=0.1$ and very low temperatures ($g=100$). There are two regimes of behavior noticeable, corresponding to $\xi^d > \xi^a$ or $\xi^a < \xi^d$.

When ξ^d is very small (for instance, $\xi^d=0.01$), the critical ac density $\xi_c^a(\xi^d=0.01)$ is found to be equal to $A \approx 1$ [see Fig. 5(a)]. When the dc drive current density ξ^d is smaller than A (i.e., $0 < \xi^d < A$), it can be seen that the ac critical current density ξ_c^a as a function of ξ^d decreases and that both the step size and step rising pattern are changed. In the inset of Fig. 5(a) we plot the ξ_c^a as a function of ξ^d for $\Omega=0.1$. A linear fit $\xi_c^a = -\xi^d + A$ yields $A=1.02$. Note, however, that this $\xi_c^a(\xi^d)$ function is weakly frequency dependent.

When $\xi^d > A$, initially apparent jumps appear and with further increase in the ac drive current density ξ^a , the ρ_1 begins to decrease with smoothed intermittent steps and eventually approaches the unity. This regime ($\xi^a, \xi^d > \xi_c^a$) is rather interesting because it shows strong vortex-locking effects in the ac impedance, similar to the Shapiro steps seen in the dc CVCs. For very large values of ξ^d ($\xi^d=10$), as expected, the effect of the microwave current density is negligible and the ac dimensionless resistivity ρ_1 approaches unity.

In the case of ac reactivity ζ_1 , which is plotted in Fig. 5(b), the smoothed x jump is not affected by the increase in the dc density ξ^d . However, the amplitude of this jump reduces substantially for larger values of ξ^d .

In Fig. 6 we plot ρ_1 and ζ_1 versus ξ^d for different ac drive current densities, $\xi^a=0.01, 0.1, 0.5, 0.7, 1.5, 10$. It can be observed from Fig. 6(a) that for all values of ξ^a , as ξ^d increases, ρ_1 initially increases, reaches a maximum (very narrow and high for $\xi^a \leq 0.1$), and approaches unity eventually. On the other hand, ζ_1 decreases for $\xi^a \leq 0.1$, slowly increases below $\xi^d \leq 1$, and then sharply decreases, having in the vicinity of $\xi^d \approx 1$ a deep minimum, and then approaches zero. So the occurrence of the x jump can be seen clearly when ξ^d is small, whereas large values of either ξ^a or ξ^d diminish the effect of the x jumps.

In Fig. 6(a) the $\rho_1(\xi^d)$ dependences demonstrate several main features. First, the curves calculated at $\xi^a \ll 1$ show the progressive shrinking of the flux creep range [where $\rho_1(\xi^d) \ll 1$] with increasing ξ^a . If we define the $\xi_c^d(\xi^a)$ as the dependence of the dc critical current on the value of a small ac drive, then we can show that $\xi_c^d \approx 1 - \xi^a$ at $\xi^a \ll 1$. The physical reason for such behavior is obvious. Second, the appearance of a high peak in $\rho_1(\xi^d)$ near $\xi^d=1$ for $\xi^a \rightarrow 0$ can be simply explained from an examination of the dc CVC curves, calculated at $\xi^a \rightarrow 0$. In this limit it is evident that a *dynamic* dc resistivity (taken in the vicinity of the ξ_c^d), which is equal to the derivative of the dc CVC with respect to the ξ^d , is strongly enhanced at $T \rightarrow 0$. Third, taking into account an analogy between Brownian motion in a tilted periodic potential and continuous phase transitions,²⁶ one can say that a thresholdlike phase transition in the vortex motion along the x axis occurs between the “localized” vortex state at $\xi^d < \xi_c^d(\xi^a)$ and the “delocalized” running state at $\xi^d > \xi_c^d(\xi^a)$. If we consider only the *linear* impedance response [i.e., $Z_{1,L}(\omega)$ does not depend on ξ^a], this phase transition takes place at $\xi^d=1$ and at the x point²⁶ where $d^2U_p/dx^2=0$. Fourth, as was shown recently in Ref. 18, a strong enhancement of the effective diffusion coefficient D of an overdamped Brownian

particle in a tilted washboard potential near the critical tilt may occur; that, in our case, $D(\xi^d)$ may have a peak in the vicinity of $\xi^d=1$.

The consequences of the D enhancement we analyze with the aid of Fig. 7, where the frequency dependence of $\rho_1(\Omega|\xi^d=0)$ (monotonic curves) and $\rho_1(\Omega|\xi^d=1)$ (nonmonotonic curves) calculated at $\xi^a=0$ for three different temperatures ($g=10, 20, 50$) are shown. The monotonic curves $\xi^d=0$ agree with the results of Coffey and Clem,¹¹ who, in fact, calculated the temperature dependence of the depinning frequency (introduced at $T=0$ in Ref. 10) in a *nontilted* cosine pinning potential. In contrast to this monotonic behavior, the nonmonotonic curves ($\xi^d=1$) demonstrate two characteristic features: first, an anomalous power absorption ($\rho_1 \approx 1.6-2.8$) at very low frequencies and second, a deep minimum for the power absorption ($\rho_1 \approx 0.3-0.6$) at T -dependent Ω_{\min} . The appearance of this frequency- and temperature-dependent minimum at $\xi^d=1$ may be related to the resonance activated reduction in the mean escape time of the Brownian particle due to an oscillatory variation of the pinning barrier height.²⁷

At last we consider the frequency dependence of the k th transformation coefficient amplitude, i.e., $|Z_k|(\Omega|j^d, j^a, g)$ taken at different values of the dc and ac densities and inverse temperature. Here we point out only the summary of the $|Z_k|(\Omega)$ curves' behavior because a more detailed description of these results (interesting for applications) will be published elsewhere.

The main feature of the frequency dependence of the k th harmonics is the appearance (see Fig. 8) of a pronounced maximum at $\xi^d=1$ for $\Omega_{\max}=0.1$ in both $\text{Re } Z_k(\Omega)$ and $|Z_k|(\Omega)$ curves. The magnitude of the maximum is increasing with ξ^a decreasing to zero and g increasing to infinity. For example, the magnitudes of $\text{Re } Z_k(\Omega_{\max})$ and $|Z_k|(\Omega_{\max})$ are approximately equal to 20 for $k=3, 4$ at $g=30$, $\xi^d=1$, and $\xi^a=0.01$. The emergence of this maximum and its growth with the temperature decrease ($g \rightarrow \infty$) is related to the origin of a singularity of the $\delta'(\omega)$ type in the Ω dependence of the linear impedance response of the overdamped shunted Josephson junction at $T=0$ and $\xi^d \leq 1$.²⁸ Note also that $\text{Re } Z_k(\Omega)$ becomes negative in the vicinity of Ω_{\max} , which, in turn, is related to the origin of a similar singularity in the linear $Z_1(j^{dc}|\Omega, g)$ response with the increasing Ω .

VI. CONCLUSION

In conclusion, the considered exactly solvable two-dimensional model of the vortex dynamics is of great interest since very rich physics is expected from combination of a strong dc and ac drive, arbitrary value of the Hall effect [note that a big Hall effect was observed in YBCO (Ref. 29)], and the low-temperature-mediated vortex hopping (or running) in a washboard pinning potential. The obtained findings substantially generalize previous theoretical results in the field of the dc (Refs. 2 and 3) and ac (Refs. 11–13) stochastic approach to the study of the vortex dynamics in the washboard planar pinning potential. Experimental realization of this model in thin-film geometry^{8,9} opens up the possibility of carrying out a variety of experimental studies of directed

motion of vortices under (dc+ac) drive simply by measuring longitudinal and transverse voltages. Experimental control of a frequency and value of the driving forces, damping, Hall constant, pinning parameters, and temperature can be effectively provided.

While the discussion in this paper has been entirely in the context of nonlinear 2D pinning-mediated vortex dynamics, we are aware that obtained results are generic to all systems with a tilted washboard potential subjected to an ac drive. In this sense we are conscious of that physical explanation of our results should be supplemented with several new notions widely discussed. Here we mean notions of stochastic resonance,³⁰ resonance activation,²⁷ and noise enhanced stability³¹ which may be used not only for interpretation of our theoretical results but, on the contrary, the experimental verification of some predictions of these new approaches may be performed with the aid of the model under discussion.

It was shown also how pronounced nonlinear effects appear in the ac response and the linear-response solutions are recovered from the nonlinear ac response in the weak ac limit. The influence of a subcritical or overcritical dc on the time-dependent stationary ac longitudinal and transverse resistive vortex response (on the frequency of an ac drive Ω) in terms of the nonlinear impedance tensor \hat{Z} and a nonlinear ac

response at Ω harmonics are studied. Analytical formulas for 2D temperature-dependent *linear* impedance tensor \hat{Z}_L in the presence of a dc which depend on the angle α between the current-density vector and the guiding direction of the washboard PPP are derived and analyzed. Influence of α anisotropy and the Hall effect on the nonlinear power absorption by vortices is pointed out.

Up to now we have considered only the vortex motion problem. For the future experimental verification of our theoretical findings, we should keep in mind that they may be applied directly only for thin-film superconductors in the form of naturally grown (for example, in the untwined *a*-axis-oriented YBCO film³²) and artificially prepared washboard pinning structures.⁸ An application of our results for more general cases should take into account that they may be supplemented by consideration of the complex penetration length and the quasiparticle contribution in the way as it was made in the papers.^{11,33}

ACKNOWLEDGMENTS

We would like to acknowledge Yu. P. Kalmykov for chapters 2 and 5 of the book *The Langevin Equation* kindly sent. The work of O.V.D. was supported in part by I. E. Tarapov research grant of the Kharkov National University.

-
- ¹G. Blatter, M. V. Feigelman, V. B. Geshkenbein, A. I. Larkin, and V. M. Vinokur, *Rev. Mod. Phys.* **66**, 1125 (1994).
²Y. Mawatari, *Phys. Rev. B* **56**, 3433 (1997); **59**, 12033 (1999).
³V. A. Shklovskij, A. A. Soroka, and A. K. Soroka, *Zh. Eksp. Teor. Fiz.* **116**, 2103 (1999) [*JETP* **89**, 1138 (1999)].
⁴V. A. Shklovskij and O. V. Dobrovolskiy, *Phys. Rev. B* **74**, 104511 (2006).
⁵V. V. Chabanenko, A. A. Prodan, V. A. Shklovskij, A. V. Bondarenko, M. A. Obolenskii, H. Szymczak, and S. Piechota, *Physica C* **314**, 133 (1999).
⁶H. Pastoriza, S. Candia, and G. Nieva, *Phys. Rev. Lett.* **83**, 1026 (1999).
⁷G. D'Anna, V. Berseth, L. Forro, A. Erb, and E. Walker, *Phys. Rev. Lett.* **81**, 2530 (1998).
⁸M. Huth, K. A. Ritley, J. Oster, H. Dosch, and H. Adrian, *Adv. Funct. Mater.* **12**, 333 (2002).
⁹O. K. Soroka, V. A. Shklovskij, and M. Huth, *Phys. Rev. B* **76**, 014504 (2007).
¹⁰J. I. Gittleman and B. Rosenblum, *Phys. Rev. Lett.* **16**, 734 (1966).
¹¹M. W. Coffey and J. R. Clem, *Phys. Rev. Lett.* **67**, 386 (1991).
¹²M. Martinoli, Ph. Fluckiger, V. Marsico, P. K. Srivastava, Ch. Leemann, and J. L. Gavilano, *Physica B (Amsterdam)* **165-166**, 1163 (1990).
¹³M. Golosovsky, Y. Naveh, and D. Davidov, *Phys. Rev. B* **45**, 7495 (1992).
¹⁴W. T. Coffey, Yu. P. Kalmykov, and J. T. Waldron, *The Langevin Equation*, 2nd ed. (World Scientific, Singapore, 2004), Chap. 5.
¹⁵W. T. Coffey, J. L. Dejardin, and Yu. P. Kalmykov, *Phys. Rev. B* **62**, 3480 (2000).
¹⁶H. Risken, *The Fokker-Planck Equation*, 2nd ed. (Springer, Berlin, 1989).
¹⁷G. N. Watson, *Theory of Bessel Functions*, 2nd ed. (Cambridge University Press, Cambridge, England, 1944), p. 46.
¹⁸P. Reimann, C. Van den Broeck, H. Linke, P. Hanggi, J. M. Rubi, and A. Perez-Madrid, *Phys. Rev. Lett.* **87**, 010602 (2001).
¹⁹H. Kanter and F. L. Vernon, *J. Appl. Phys.* **43**, 3174 (1972).
²⁰L. G. Aslamazov and A. I. Larkin, *Zh. Eksp. Teor. Fiz. Pis'ma Red.* **9**, 150 (1968) [*JETP Lett.* **9**, 87 (1969)].
²¹K. K. Likharev and B. T. Ulrich, *Systems with Josephson Contacts* (MSU, Moscow, 1978).
²²C. Vanneste *et al.*, *Phys. Rev. B* **31**, 4230 (1985).
²³Z. Zhai, P. V. Parimi, and S. Sridhar, *Phys. Rev. B* **59**, 9573 (1999).
²⁴J. McDonald and J. R. Clem, *Phys. Rev. B* **56**, 14723 (1997).
²⁵L. M. Xie, J. Wosik, and J. C. Wolfe, *Phys. Rev. B* **54**, 15494 (1996).
²⁶O. V. Usatenko and V. A. Shklovskij, *J. Phys. A* **27**, 5043 (1994).
²⁷M. Boguna, J. M. Porra, J. Masoliver, and K. Lindenberg, *Phys. Rev. E* **57**, 3990 (1998).
²⁸F. Auracher and T. van Duzer, *J. Appl. Phys.* **44**, 848 (1973).
²⁹J. M. Harris, Y. F. Yan, O. K. C. Tsui, Y. Matsuda, and N. P. Ong, *Phys. Rev. Lett.* **73**, 1711 (1994).
³⁰L. Gammaitoni, P. Hänggi, P. Jung, and F. Marchesoni, *Rev. Mod. Phys.* **70**, 223 (1998).
³¹R. N. Mantegna and B. Spagnolo, *Phys. Rev. Lett.* **76**, 563 (1996).
³²Z. Trajanovic, C. J. Lobb, M. Rajeswari, I. Takeuchi, C. Kwon, and T. Venkatesan, *Phys. Rev. B* **56**, 925 (1997).
³³E. Silva, N. Pompeo, S. Sarti, and C. Amabile, in *Recent Developments in Superconductivity Research*, edited by B. P. Martins (Nova Science, Hauppauge, NY, 2006), pp. 201–243.